The Journal of Toxicological Sciences (J. Toxicol. Sci.)
Vol.34, Special Issue II, SP279-SP286, 2009

Intrauterine environment-genome interaction and Children's development (2): Brain structure impairment and behavioral disturbance induced in male mice offspring by a single intraperitoneal administration of domoic acid (DA) to their dams

Kentaro Tanemura, Katsuhide Igarashi, Toshiko-R Matsugami, Ken-ichi Aisaki, Satoshi Kitajima and Jun Kanno

Division of Cellular & Molecular Toxicology, Biological Safety Research Center, National Institute of Health Sciences, 1-18-1 Kamiyoga, Setagaya-ku, Tokyo 158-8501, Japan

(Received February 17, 2009)

ABSTRACT — To demonstrate induction of delayed central nervous toxicity by disturbing neuronal activities in the developing brain, we administered a single intraperitoneal dose of domoic acid (DA; 1 mg/kg), a potent glutamate receptor agonist, to pregnant female mice at the gestational day of 11.5, 14.5 or 17.5. The dams had recovered from acute symptoms within 24 hr, followed by normal delivery, feeding and weaning. All male offspring mice after weaning were apparently normal in response to handlers during cage maintenance, body weight measurement and to mate mice in group housing conditions. At the age of 11 weeks, our neurobehavior testing battery revealed severe impairment of learning and memory with serious deviances of anxiety-related behaviors. The developed brain of prenatally exposed mice showed myelination failure and the overgrowth of neuronal processes of the limbic cortex neurons. This study indicates that the temporal disturbance of neurotransmission of the developing brain induces irreversible structural and functional damage to offspring which becomes monitorable in their adulthood by a proper battery of neurobehavioral tests.

Key words: Domoic acid, Prenatal exposure, Brain structure, Behavior

INTRODUCTION

Adequate neural activities are necessary for the maturation of neural networks during brain development (Rice and Barone, 2000). Historically, the presence of such plasticity-driven mechanisms has been demonstrated by a series of studies of eyelid suture in kittens or monkeys and corresponding findings reported in young human cataracta patients (Wiesel, 1982; Gu *et al.*, 1989; Fonta *et al.*, 2000). These processes require proper stimuli to the brain that trigger the release of neurotransmitters from the neurons and subsequent receptor-mediated signal transduction (Ooi and Wood, 2008; Greer and Greenberg, 2008; Cohen-Cory, 2002). Therefore, it is highly conceivable that disturbance of neural activities by neuroactive xenobiotics leads to malformation of the fine structure of the brain. Even when the exposure was transient, it would result in anomaly of higher brain functions in adulthood without overt signs of brain damage during maturation.

Glutamate receptors begin to express in the late embryonic stages, and their expression increases with the advance of brain development (Luján *et al.*, 2005; Manent *et al.*, 2005). Prenatal exposure of xenobiotic chemicals that interfere with the glutamate receptor function could induce malformation of the fine structure of the brain which should lead to anomaly of higher brain function that is different from acute neurotoxicity known for such chemicals to induce in adults (Bondy and Campbell, 2005). A marine biotoxin domoic acid (DA) which is structurally related to glutamate, and activates ionotropic α-amino-3-hydroxy-5-methyl-4-isoxazolepropionic acid (AMPA) and kinate subtypes of glutamate receptors (Pulido, 2008) is known to cause acute symptoms of diarrhea, seizures and memory loss in adult human by eating contaminated shellfish (Tryphonas and Iverson, 1990), and DA induced acute neurotoxicity in animal

Correspondence: Jun Kanno (E-mail: kanno@nihs.go.jp)

model (Chandrasekaran *et al.*, 2004). Additionally, DA is also known to cross the placenta, and enters prenatal brain tissue in rats (Maucher and Ramsdell, 2007). Therefore, prenatal exposure of DA may disrupt the neural activities by excessive stimulation of glutamate receptors, and should induce fine structural and functional disorganization in the developing brain. Here, we report that a transient transplacental DA exposure *in utero* induced alteration of the neurobehavioral parameters and corresponding fine brain structure of the male C57BL/6 mice in their adulthood.

MATERIALS AND METHODS

Animal treatment

All experiments were carried out under approval of Experimental Animal Use Committee of National Institute of Health Sciences, Japan. Pregnant C57LB/6 female mice obtained from Japan SLC, Inc., were individually housed in plastic breeding cages with free access to water and pellet diet (CRF-1; Oriental Yeast Co., Tokyo, Japan) in a 12 hr light-dark cycle conventional condition. Four groups with five pregnant mice each were prepared. All groups received three intraperitoneal injections on gestational day 11.5 (E11.5) as a late embryonic period, 14.5 (E14.5) and 17.5 (E17.5) as early and late fetal period respectively. Group A (Control) received three i.p. shots of saline on E11.5, E14.5 and E17.5. Group B (DA@E11.5) received one shot of DA (Calbiochem, San Diego, CA, USA) at a dosage of 1 mg/kg on E 11.5 and two shots of saline on E14.5 and E17.5. Group C (DA@14.5) received a shot of saline on E11.5, a shot of DA on E14.5 and another saline on E17.5. Group D (DA@E17.5) received two shots of saline on E11.5 and E14.5 , and a shot of DA on E17.5. The pups were weaned at 4 weeks of age, and four male mice per liter were randomly selected and housed in one cage with free access to water and CRF-1 pellet until 11 weeks of age.

Immunohistochemical analysis

Brains (n = 4 male mice per group) were fixed with methacarn fixative (methanol: chloroform:acetic acid, 60:30:10 v/v) and paraffin-embedded sections were prepared. Mouse monoclonal anti-microtubule associated protein 2 (MAP2, sc-32791; Santa Cruz, CA, USA), mouse monoclonal anti-neurofilament-m (NF-M, sc-20013; Santa Cruz, CA, USA), rabbit polyclonal anti-myelin associated glycoprotein (MAG, sc-15324; Santa Cruz, CA, USA), and rabbit polyclonal anti MAP2 (sc-20172; Santa Cruz, CA, USA) were used. Deparaffinized sections were pretreated with HistoVT-One (Nacalai Tesque, Kyoto, Japan.) as previously described (Tanemura *et al.*, 2005) and incubated with primary antibodies. Secondary antibodies were Alexa 568-conjugated anti-mouse IgG and Alexa 488-conjugated anti-rabbit IgG (Molecular Probes, Eugene, OR, USA). Fluorescent images were obtained with an FV-300 confocal laser scanning microscope (Olympus, Tokyo, Japan). For semi-quantitative analysis of images, we calculated the ratio of fluorescence intensity compared to control mice (group A), by using the IMAGE J program (http://rsb.info.nih.gov/ij/index.html. National Institute of Health, Bethesda), after adjusting background noise (n = 4 images per mouse).

Neurobehavioral tests

A battery of neurobehavioral tests were conducted on open field test (OF), light/dark transition test (LD), elevated plus maze test (EP) and contextual/cued fear conditioning test (FZ). Experimental apparatuses and image analyzing softwares were obtained from O'Hara & Co., Ltd., Japan. Image analyzing softwares (Image OF4, Image LD2, Image EP2 and Image FZ2) were developed from the public domain IMAGE J program. All experiments were done with 8 mice per group (32 mice total), and were conducted between 13:30 and 16:30. The level of background noise during behavioural testing was about 50 dBA. After each trial, the apparatuses were wiped and cleaned.

Open field test

The locomotor activity was measured for 10 min using an open field apparatus made of white plastic (50 x 50 x 40 (H) cm).

An LED light system was positioned 50 cm above the centre of the field (50 lux at the centre of field). Total distance travelled (cm), time spent in the central area (30% of the field) (sec), and the frequencies of movement were measured (Tanemura *et al.*, 2002).

Light/dark transition test

The apparatus used for the light/dark transition test consisted of a cage (21 x 42 x 25(H) cm) divided into two chambers by a partition with an opening. One chamber is brightly illuminated (250 lux), whereas the other chamber is dark (2 lux). A mouse is placed into the dark area and allowed to move freely between the two chambers through the opening for 5 min. The latency for the first move to the light area, the total number of transitions and the time spent on each side were measured.

Elevated plus maze test

The plus-shaped apparatus consisted of four arms (25

x 5 cm) connected to a central square area (5 x 5 cm). Opposite two arms are enclosed with 20 cm-high transparent walls and other two are left open. The floor of the maze is made of white plastic plate and is elevated 60 cm above the room floor (200 lux at the centre of the apparatus). A mouse is placed to the central square area of the maze, facing one of the open arms, and the behavior was recorded for 10 min: total distance traveled (cm), total time on open arms and central square area (sec) and the total number of entry to any of the arms (Tanemura *et al.*, 2002).

Contextual/cued fear conditioning test

The apparatus consists of a conditioning chamber (or a test chamber) (17 x 10 x 10 (H) cm) made of clear plastic with ceiling and placed in a sound proof box. The chamber floor has stainless steel rods (2-mm diameter) spaced 5 mm apart for giving electric foot shock (0.1 mA, 3 sec duration) to the mouse. The soundproof box consists of white-coloured wood, and is equipped with an audio speaker and light source (35 lux at the centre of the floor). A CCD camera is positioned 20 cm above the ceiling of the chamber. During the conditioning trial (Day 1), mice are placed individually into the conditioning chamber in the sound proof box and, after 90 sec, they are given three tone-shock pairings (30 sec of tone, 75 dB, 10 KHz followed by 3 sec of electric shock at the end of tone, 0.1 mA) separated by 90 sec. Then they are returned to their home cage. Next day (Day 2), as a "contextual fear test", they are returned to the conditioning chamber without tone and shock for a 6-min. On the third day (Day 3), they are brought to a novel chamber of different make without stainless steel rods place in the sound proof box and, after a period of 3 min, only the conditioning tone is presented for 3 min (no shock was presented, 35 lux at the centre of the floor). The freezing response of mice was defined as a consecutive 2 sec period of immobility. Freezing rate (%) was calculated as [time freezing/session time] x 100 (Tatebayashi *et al.*, 2002).

Statistical analysis

Data were indicated as means ± S.D. Statistical analysis was conducted with student's t-test by using StatView (SAS Institute, Cary, NC, USA). A p-value of < 0.05 compared to the results of control male mice (group A) was considered statistically significant.

RESULTS

Effects on morphology of brain by prenatal exposure to DA

Offspring mice of all groups after weaning up to the age of 11 weeks were apparently normal in response to handlers during cage maintenance, body weight measurement and to mate mice in group housing conditions. Routine histological observation of the brain at 11 weeks old by hematoxylin-eosin staining could not reveal difference among the groups (data not shown). By immunohistochemical study on the same brain sections, reduced immuno-reactivity against the MAG, the marker for myelin, was detected in the cortices of group B (DA@11.5) and C (DA@14.5) compared to control (Figs. 1A-D and I). In contrast, increased immuno-reactivity against MAP2, the marker for neuronal dendrite, was indicated in the same area of group B (DA@11.5), C (DA@14.5) and D (DA@17.5) compared to control (Figs. 1E-H and J). Increased immuno-reactivity against MAP2 was also found in lateral area of CA3 hippocampus of group B (DA@11.5), C (DA@14.5) and D (DA@17.5) compared to control, whereas immuno-reactivity for MAP2 showed no significant difference in medial area of CA3 hippocampus among the groups (Figs. 2A-D and I). Immuno-reactivity against NF-M; the marker for neuronal axon, also showed no significant difference in the same area among the groups (Figs. 2E-H and J).

Effects on behavior by prenatal exposure of DA

In the OF test, the distance traveled was not different among the groups (Fig. 3A), the time spent in center area was significantly prolonged in group D (DA@17.5) mice (Fig. 3B). In the LD test, group C (DA@14.5) mice stayed in light area for longer time (Fig. 4A), and latency for the first move to light area was significantly shorter in group C (DA@14.5) and D (DA@17.5) (Fig. 4B). In the EP test, significantly increased distance traveled and time spent in the open area were detected for group B (DA@11.5), C (DA@14.5) and D (DA@17.5) (Figs. 5A and B). In the FZ test, both Day 1 and Day 2 freezing responses of group C (DA@14.5) and D (DA@17.5) were significantly reduced compared to control (Figs. 6A and B).

DISCUSSION

The expression levels of glutamate receptors starts to elevate at the fetal period, i.e. approximately from E14 (Luján *et al.*, 2005; Manent *et al.*, 2005). Exogenous glutamatergic stimuli at this period would affect the for-

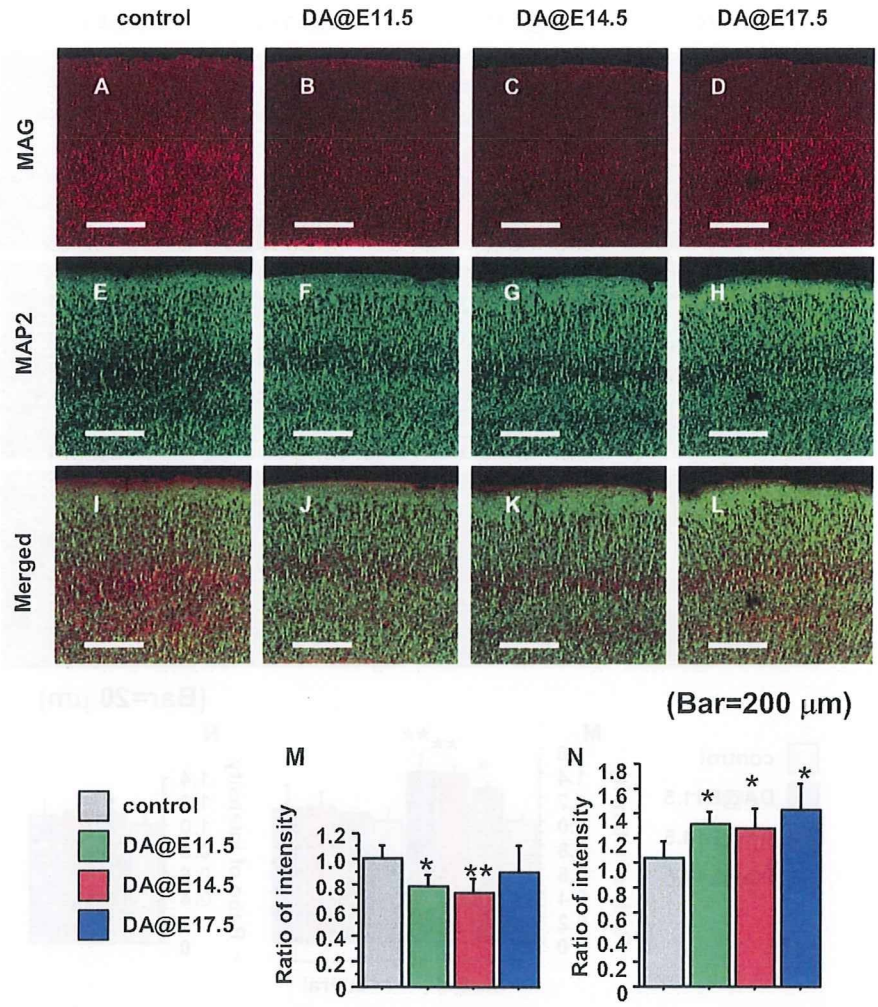

Fig. 1. Delayed effects on cerebral cortex induced by prenatal exposure of DA.
A-D, Immunohistochemical staining against MAG; E-H, immunohistochamical staining against MAP2; I-L, merged images of the cerebral cortex. A, E, I, group A (control), B, F, J, group B (DA@11.5), C, G, K, group C (DA@14.5) and D, H, L, group D (DA@17.5). Scale bar = 200 mm. M, Quantitative analysis in intensity ratio to control of MAG expression, and J, MAP2 expression among the groups (mean ± S.E.M.). Asterisk (**) and (*) indicate significant difference compared to control ($P < 0.01$) and ($P < 0.05$).

mation of the neural circuits. An extreme example to support this hypothesis would be the phenotype of the double knockout mouse of glutamate transportors GLT1 and GLAST (Matsugami *et al.*, 2006). Lack of these transportors is considered to result in abnormally high concentration of glutamate in the brain. In fact, morphological anomaly became apparent in synchronization with the expression of glutamine receptors. In our study, corresponding to the hypothesis, the neurobehavioral symptoms as a whole was severer for those exposed at fetal periods, i.e. E14.5 and E17.5, compared to those at embryonic period, i.e. E11.5 (Fig. 7).

We demonstrated that a prenatal exposure of a relatively low dose of DA induced a spectrum of neurobehavioral anomalies which became monitorable at the adult stage accompanied by alteration in fine brain structures detectable by immunohistochemistry. It is emphasized that this amount of DA did not induce abnormal responses dur-

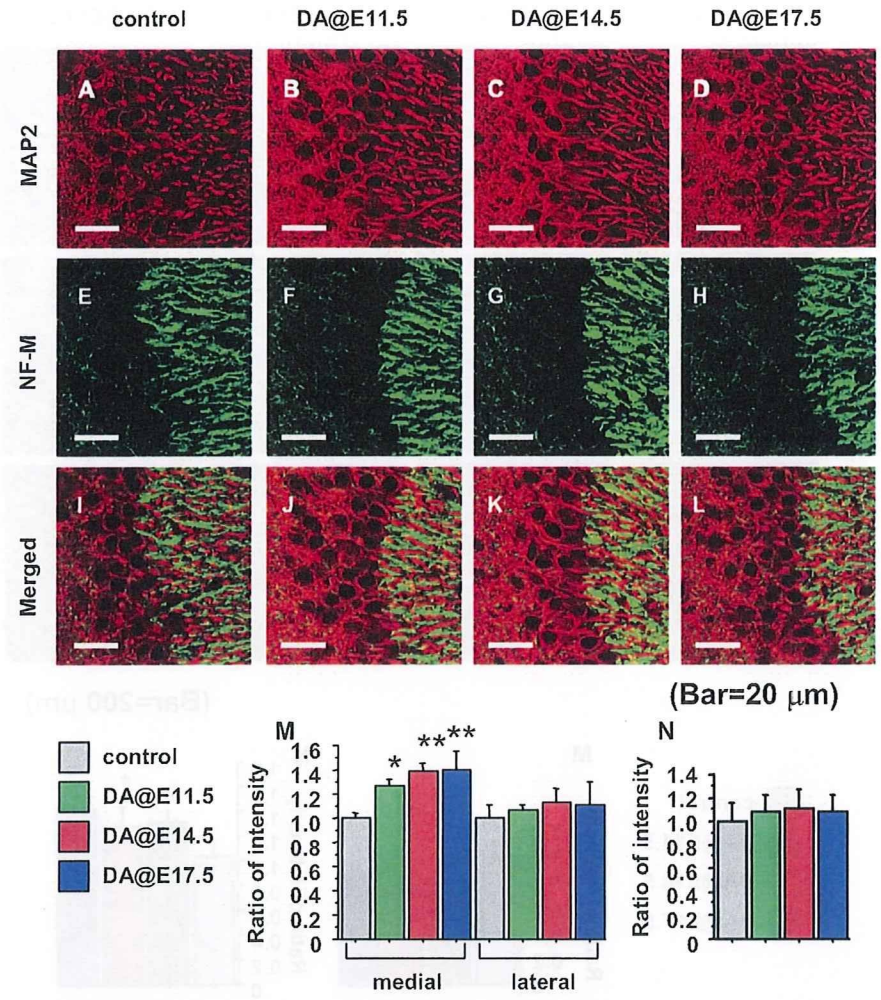

Fig. 2. Delayed effects on hippocampus induced by prenatal exposure of DA.
A-D, Immunohistochemical staining against MAP2; E-H, immunohistochamical staining against NF-M; I-L, merged images, of CA3 hippocampus. A, E, I, group A (control), B, F, J, group B (DA@11.5), C, G, K, group C (DA@14.5) and D, H, L, group D (DA@17.5). Scale bar = 200 mm. M, Quantitative analysis of MAP2 expression, and N, NF-M expression among the groups (mean ± S.E.M.). Asterisk (**) and (*) indicated significant difference compared to control ($P < 0.01$) and ($P < 0.05$).

ing maturation, such as hyperreactivity to handling and to cage mates, and did not present overt malformation of the brain detectable by the routine H&E histology at the age of 2 weeks (data not shown). It is also noted that the spectrum of the neurobehavioral symptoms induced in mice exposed to DA at adulthood was different from those monitored in this study (data not shown).

Although progressive hippocampal neuronal damages were reported to be induced by prenatal administration of DA (0.6 mg/kg intravenous injection to the dam) (Dakshinamurti *et al.*, 1993), we did not find notable neuronal loss or neuronal cell death as the delayed effects in adult mouse brain by prenatal exposure. On the other hand, we found myelination failure (Miller and Mi, 2007) in cortex of group B (DA@11.5) and C (DA@14.5) mice. And we also detected a finding compatible with the overgrowth of neuronal processes in cortex and hippocampus of group B (DA@11.5), C (DA@14.5) and D (DA@14.5)

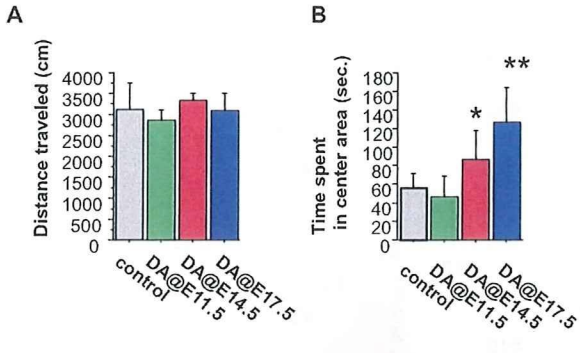

Fig. 3. Delayed effects on locomotor activity (OF test) induced by prenatal exposure of DA.
A, Mean distance travelled (total distances divided by total duration of trial, 10 min) and B, mean time spent in center area (30% of the field) in the open field apparatus (mean ± S.E.M.). Asterisk (**) and (*) indicated significant difference compared to control ($P < 0.01$) and ($P < 0.05$).

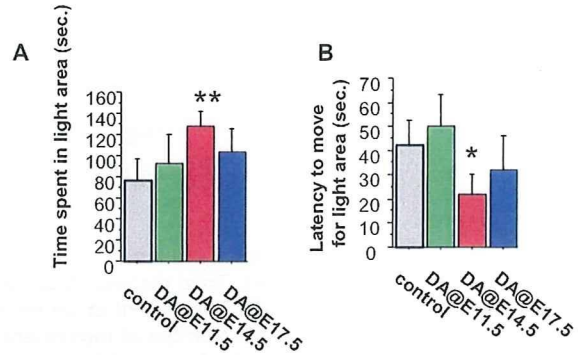

Fig. 4. Delayed effects on anxiety-related behavior (LD test) induced by prenatal exposure of DA.
A, Total time spent in light area, and B, latency time to move to light area in the LD apparatus (mean ± S.E.M.). Asterisk (**) and (*) indicated significant difference compared to control ($P < 0.01$) and ($P < 0.05$).

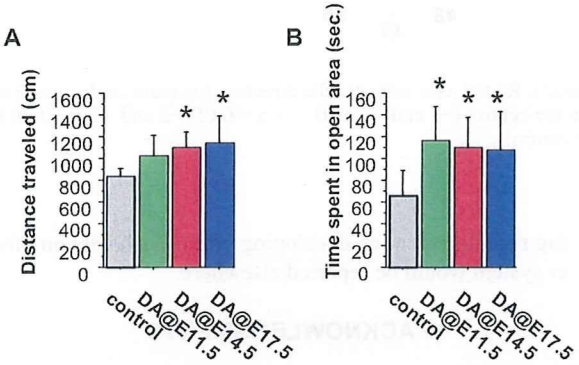

Fig. 5. Delayed effects on anxiety-related behavior (EP test) induced by prenatal exposure of DA.
A, Total distance travelled, and B, total time spent in open area in the elevated plus maze apparatus (mean ± S.E.M.). Asterisk (*) indicated significant difference compared to control ($P < 0.05$).

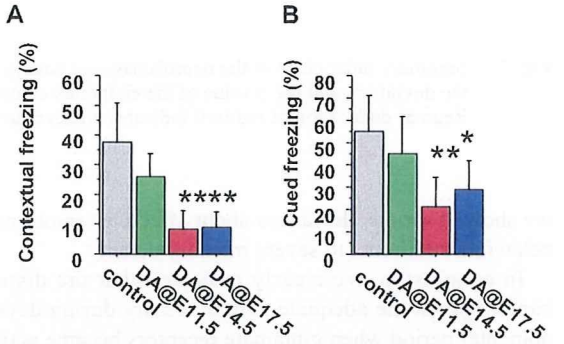

Fig. 6. Delayed effects on learning and memory (FZ test) induced by prenatal exposure of DA.
A, Contextual fear test and B, cued fear test. Memory performance is expressed as a mean percent duration of freezing responses (mean ± S.E.M.). Asterisk (**) and (*) indicated significant difference compared to control ($P < 0.01$) and ($P < 0.05$).

mice by using cytoskeletal marker. These findings indicated that the disorganization of brain was induced by the prenatal exposure of DA, and remained irreversibly up until the maturation period.

Among multiple endpoints of the behavioral test battery we used, serious deviances in anxiety-related behaviors of group C (DA@14.5) and D (DA@17.5) mice were observed. Mice in those groups showed low performances in adaptations for novel circumstances, i.e., strange and broad area in OF test, beamish place in LD test, high and narrow space in EP test. Additionally, we also found severe impairment of learning and memory. Although the low performances of memory task have been reported in rats with prenatal DA exposure (Levin *et al.*, 2005),

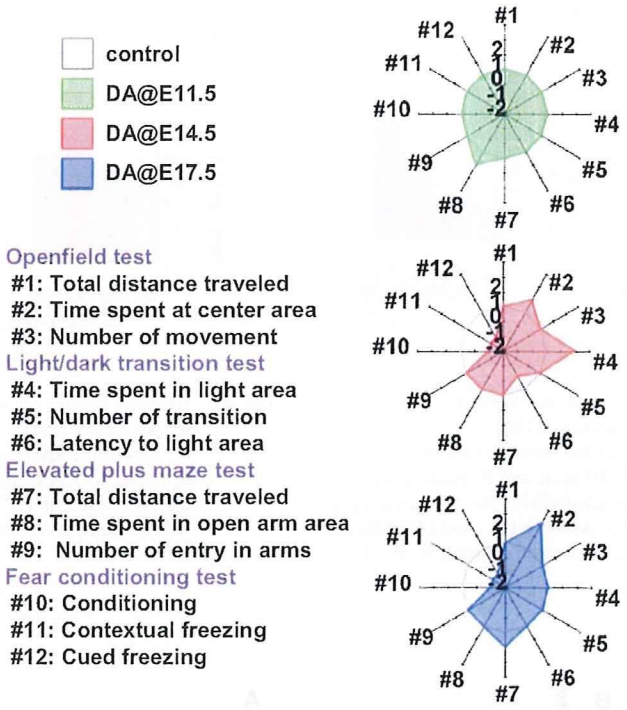

Fig. 7. Summary radar chart of the neurobehavioral battery test results. Radial axis indicates the direction (increase or decrease) of the deviation, and the p value of the endpoints compared to the control (+1 and −1, $0.01 <= p < 0.05$, +2 and −2, $p < 0.01$). Regular dodecagon of radius 0 indicates no deviation from control.

we showed serious deviances about affective (emotional) behaviors additional to severe memory deficit.

In conclusion, we clearly indicated that the disturbance against the adequate neural activity during developmental period when glutamate receptors became active have induced delayed memory defect and unnatural adoptive behaviors that became monitorable at the maturation period in mice. The responsible foci deduced from these behavioral disturbances are the limbic cortex and hippocampus. Our morphological findings are consistent with the interpretation. A combination of neurobehavioral and pathomorphological analysis was shown to be an effective method to assess delayed neurotoxic effects which dose not induce immediate organic brain damage and related symptoms after exposure. Having adopted the hypothesis that exogenous stimuli to neural signaling systems during the development of the brain can be a cause of delayed anomaly of higher brain function, stimuli toward systems other than glutamate receptors should also induce such anomaly of different targets and symptoms in concert with the distribution of the corresponding receptor(s) in the developing brain. Such data on other system would be reported elsewhere.

ACKNOWLEDGMENTS

The authors thank Mr. Yusuke Furukawa and Ms. Maki Otsuka for technical support. This study was supported by Health Sciences Research Grants H17- -Kagaku- 001 from the Ministry of Health, Labour and Welfare, Japan.

This peer-reviewed article is based upon a lecture presented at the 35th Annual Meeting of Japanese Society of Toxicology, June 2008 in Tokyo under the theme of "Children's Toxicology", June 2008 in Tokyo.

REFERENCES

Bondy, S.C. and Campbell, A. (2005): Developmental neurotoxicology. J. Neurosci. Res., **81**, 605-612.

Chandrasekaran, A., Ponnambalam, G. and Kaur, C. (2004): Domoic acid-induced neurotoxicity in the hippocampus of adult rats. Neurotox. Res., **6**, 105-117.

Cohen-Cory, S. (2002): The developing synapse: construction and

modulation of synaptic structures and circuits. Science, **298**, 770-776.

Dakshinamurti, K., Sharma, S.K., Sundaram, M. and Watanabe, T. (1993): Hippocampal changes in developing postnatal mice following intrauterine exposure to domoic acid. J. Neurosci., **13**, 4486-4495.

Fonta, C., Chappert, C. and Imbert, M. (2000): Effect of monocular deprivation on NMDAR1 immunostaining in ocular dominance columns of the marmoset Callithrix jacchus. Vis. Neurosci., **17**, 345-352.

Greer, P.L. and Greenberg, M.E. (2008): From synapse to nucleus: calcium-dependent gene transcription in the control of synapse development and function. Neuron, **59**, 846-860.

Gu, Q.A., Bear, M.F. and Singer, W. (1989): Blockade of NMDA-receptors prevents ocularity changes in kitten visual cortex after reversed monocular deprivation. Brain Res. Dev. Brain Res., **47**, 281-288.

Levin, E.D., Pizarro, K., Pang, W.G., Harrison, J. and Ramsdell, J.S. (2005): Persisting behavioral consequences of prenatal domoic acid exposure in rats. Neurotoxicol. Teratol., **27**, 719-725.

Luján, R., Shigemoto, R. and López-Bendito, G. (2005): Glutamate and GABA receptor signalling in the developing brain. Neuroscience, **130**, 567-580.

Manent, J.B., Demarque, M., Jorquera, I., Pellegrino, C., Ben-Ari, Y., Aniksztejn, L. and Represa, A. (2005): A noncanonical release of GABA and glutamate modulates neuronal migration. J Neurosci., **25**, 4755-4765.

Matsugami, T.R., Tanemura, K., Mieda, M., Nakatomi, R., Yamada, K., Kondo, T., Ogawa, M., Obata, K., Watanabe, M., Hashikawa, T. and Tanaka, K. (2006): Indispensability of the glutamate transporters GLAST and GLT1 to brain development. Proc. Natl. Acad. Sci. USA, **103**, 12161-12166.

Maucher, J.M. and Ramsdell, J.S.(2007): Maternal-fetal transfer of domoic acid in rats at two gestational time points. Environ Health Perspect., **115**, 1743-1746.

Miller, R.H. and Mi, S. (2007): Dissecting demyelination. Nat. Neurosci., **10**, 1351-1354.

Ooi, L. and Wood, I.C. (2008): Regulation of gene expression in the nervous system. Biochem. J., **414**, 327-341.

Pulido, O.M. (2008): Domoic acid toxicologic pathology: a review. Mar. Drugs, **6**, 180-219.

Rice, D. and Barone, S.Jr. (2000): Critical periods of vulnerability for the developing nervous system: evidence from humans and animal models. Environ. Health Perspect., **108**, 511-533.

Tanemura, K., Murayama, M., Akagi, T., Hashikawa, T., Tominaga, T., Ichikawa, M., Yamaguchi, H. and Takashima, A. (2002): Neurodegeneration with tau accumulation in a transgenic mouse expressing V337M human tau. J Neurosci., **22**, 133-141.

Tanemura, K., Ogura, A., Cheong, C., Gotoh, H., Matsumoto, K., Sato, E., Hayashi, Y., Lee, H.W. and Kondo, T. (2005): Dynamic rearrangement of telomeres during spermatogenesis in mice. Dev. Biol., **281**, 196-207.

Tatebayashi, Y., Miyasaka, T., Chui, D.H., Akagi, T., Mishima, K., Iwasaki, K., Fujiwara, M., Tanemura, K., Murayama, M., Ishiguro, K., Planel, E., Sato, S., Hashikawa, T. and Takashima, A. (2002): Tau filament formation and associative memory deficit in aged mice expressing mutant (R406W) human tau. Proc. Natl. Acad. Sci. USA, **99**, 13896-13901.

Tryphonas, L. and Iverson, F. (1990): Neuropathology of excitatory neurotoxins: the domoic acid model. Toxicol Pathol., **18**, 165-169.

Wiesel, T.N. (1982): Postnatal development of the visual cortex and the influence of environment. Nature, **299**, 583-591.

Biochemical and Biophysical Research Communications 385 (2009) 319–323

Contents lists available at ScienceDirect

Biochemical and Biophysical Research Communications

journal homepage: www.elsevier.com/locate/ybbrc

Abnormalities in aggression and anxiety in transgenic mice overexpressing activin E

Kazunari Sekiyama [a], Osamu Hashimoto [a,*], Yuuki Ushiro [a], Chika Adachi [a], Takefumi Kikusui [b], Kentaro Tanemura [c], Yoshihisa Hasegawa [a]

[a] Laboratory of Experimental Animal Science, Faculty of Veterinary Medicine, Kitasato University, School of Veterinary Medicine, 35-1 Higashi 23 Bancho, Towada-shi, Aomori 034-8628, Japan
[b] Companion Animal Research, Azabu University, 1-17-1 Fuchinobe, Sagamihara-shi, Kanagawa 229-8501, Japan
[c] National Institute of Health Sciences, 1-18-1 Kamiyoga, Setagaya-ku, Tokyo 158-8501, Japan

ARTICLE INFO

Article history:
Received 21 April 2009
Available online 20 May 2009

Keywords:
Activin E
Aggression
Anxiety
Transgenic mouse

ABSTRACT

To study the function of activin E, a TGF-β superfamily member, in the regulation of affective behavior, we investigated the behavior of transgenic mice overexpressing activin E (TgActβE mice). Male TgActβE mice showed aggressive behavior in resident–intruder tests. In elevated plus-maze tests, the percentage of open arm entries was significantly increased in female TgActβE mice compared with that in wild-type mice. Furthermore, female TgActβE mice stayed in the central area for a significantly longer time than wild-type mice in open field tests. These results indicated that TgActβE mice had less anxiety-like behavior. The number of restraint-stress-evoked c-Fos-positive cells in the hypothalamic paraventricular nucleus in TgActβE mice was significantly decreased compared with that in wild-type mice. This suggests that synthesis of corticotrophin-releasing hormone induced by stress was decreased in TgActβE mice. Taking these results together, activin E may act as a regulator of the hypothalamic–pituitary–adrenal axis.

Introduction

The TGF-β superfamily has more than 30 members, including TGF-βs, growth and differentiation factors (GDFs), bone morphogenetic proteins (BMPs) and activins [1]. They carry out multifunctional regulation in a wide variety of cell and tissue types in an autocrine or paracrine manner.

Activins are disulfide-linked homo- or heterodimers of the β subunits of inhibin/activin A and B. Activin A (βAβA), activin AB (βAβB) and activin B (βBβB) were initially identified as stimulators of FSH secretion from pituitary cells [2]. However, it is now known that activins have multifunctional effects including promotion of erythroid differentiation, nerve cell survival, induction of mesoderm in *Xenopus laevis* embryos, promotion of bone growth, augmentation of somatostatin expression, and induction of cell cycle arrest and apoptosis [2].

Additional inhibin/activin β subunit genes (βC and βE) have been identified in mammals [3]. Analysis of the amino acid sequence of the mature region of known activin β subunits has indicated that the subunits have approximately 50% overall homology. The activin βC and βE subunits have the same general structure as the βA and βB subunits, with seven cysteine residues generally conserved among TGF-β superfamily members, as well as an additional two cysteines at the N-terminal region of mature proteins that are typically conserved in activins. Similar to activin βA and βB subunits, βC and βE subunits can form disulfide-linked homo- and heterodimers [3]. It has been reported that activin E is associated with cell growth and apoptosis in some cell types [3]. However, gene targeting has revealed that activin E null mice have no abnormalities so far [4]. Therefore, further study is needed to understand the function of activin E.

In the central nervous system (CNS), activins have roles in neuroprotection and antidepressant activity [5,6]. Intracerebroventricular infusion of activin A rescues neuronal damage from excitotoxic and hypoxic–ischemic brain injury. Furthermore, forebrain-specific expression of activin A leads to abnormal anxiety-related behavior [7]. These findings suggest that the regulation of activin and its signaling in the CNS are important physiologically for many aspects of behavior. Recently, aberration of mRNA expression for activins, especially activin E, has been observed in the rat brain infected with Borna disease virus (BDV), which induced abnormal behavior [8].

We have reported previously the generation and characterization of transgenic mice that overexpress human activin E [9]. It has been found that activin E plays a role in pancreatic exocrine cell growth. However, the function of activin E in the CNS is unclear. To study the role of activin E in the regulation of emotional

* Corresponding author. Fax: 81 176 23 8703.
E-mail address: ohashim@vmas.kitasato-u.ac.jp (O. Hashimoto).

0006-291X/$ - see front matter © 2009 Elsevier Inc. All rights reserved.
doi:10.1016/j.bbrc.2009.05.054

behavior, we examined transgenic mice that overexpressed activin E (TgActβE mice). We demonstrated that the mice exhibited abnormal aggressive behavior and anxiety, which suggests that activin E has a function in the brain. Furthermore, the transgenic mice may be a useful animal model for the study of mood disorders.

Materials and methods

Animals. C57BL/6 and A/J mice were obtained from SLC Japan (Hamamatsu, Japan). The generation of TgActβE mice has been described previously [9]. Two lines, 16 and 19 (TgActβE16 and TgActβE19) were backcrossed to C57BL/6 mice and analyzed together with littermate controls after 9–17 generations of backcrossing. Male mice were housed individually from the age of 8 weeks. Female mice were housed in groups of three from the age of 6 weeks. Mice were maintained in a 12-h light–dark cycle at 24 ± 2 °C and given standard chow and water *ad libitum*. Experimental procedures and the care of animals were performed in accordance with the requirements of the Institutional Animal Care Committee at Kitasato University, in compliance with National Institutes of Health guidelines.

Behavioral tests. All the behavioral experiments performed under 640-lx light conditions and were carried out between 1330 and 1630 h. Elevated plus-maze behavior was measured when mice were 9–11-weeks-old. The elevated plus-maze apparatus consisted of four arms elevated 45 cm above the floor, with each arm positioned at 90° relative to the adjacent arms. Two of the arms were enclosed with high walls (280 × 50 × 150 mm), and the other arms were open (280 × 50 mm). Open arms and closed arms were connected via a central area (50 × 50 mm) to form a plus sign. The maze was made of polypropylene and glued on cardboard. The behavior of the mice in the maze was recorded by a video camera. The camera was suspended above the maze and the experimenter was not in close proximity to the experimental setup for the duration of the study. Mice at the start of each trial were placed in the central platform of the maze, facing an open arm. A standard 5-min test was employed for each mouse. The maze was thoroughly cleaned with damp and dry towels between experimental periods. The number of entries into, and percentage of time spent in the open and closed arms were counted. Frequency and percentage of total time of other activities (self grooming, stretching, peering and rearing) were also measured in the test.

For the resident–intruder test, male TgActβE mice (14–16-weeks-old) were housed in individual cages for more than 3 weeks before testing. A male A/J mouse (8–9-weeks-old) was introduced into the cage as an intruder and we observed the aggressive confrontation. The observation was continued for 5 min after the first bite was confirmed, but when no attack took place, observation was discontinued at 10 min after introduction of the intruder. The tests were repeated twice, at 3-day intervals, for each mouse. All the experimental sessions were recorded on videotape, and the behavior parameters at the second session were scored. The durations of the following behaviors were measured: offensive biting, sideways threat, tail rattling, and jumping.

Acute stress test. TgActβE mice were stressed by restraint in a 50-ml plastic centrifuge tube for 30 min and then returned to their home cages. After 15 min, mice were anesthetized with pentobarbital (50 mg/kg, i.p. injection), venous blood samples were taken from the postcaval vein and perfused transcardially with PBS followed by Bouin's fixative. Serum corticosterone was measured using Corticosterone EIA Kits (No. 500651, Cayman Chemical, Ann Arbor, MI, USA) according to the manufacturer's instructions. The brains were subjected to histological analysis.

Histological analysis. Mice were anesthetized with pentobarbital (50 mg/kg, i.p. injection) and perfused transcardially with PBS followed by Bouin's fixative. The brain was isolated, re-fixed in Bouin's solution for 16 h and embedded in paraffin.

For detection of c-Fos, 6-μm sections of the brain were deparaffinized and heated by microwaves at an upper temperature limit of 95 °C for 30 min in 10 mM sodium citrate buffer (pH 6.0). After cooling, anti c-Fos antibody (SC-52; Santa Cruz Biotechnology, Santa Cruz, CA, USA) at a 1:500 dilution in TBS-BSA was incubated with the sections, and the immunoreactivity was visualized as described above. To quantify the c-Fos expression in the paraventricular nucleus (PVN), c-Fos-positive cells were counted in randomly selected fields (0.5 mm^2 per PVN) as described elsewhere [10].

Statistical analysis. Results were expressed as mean ± SE. Differences between groups were analyzed for statistical significance by using the χ^2 test (StatView 5.0 software; Abacus Concepts, Berkeley, CA, USA) for the resident–intruder test, multivariate analysis of variance (MANOVA) with the Hotelling–Lawley trace was conducted for the genotype and sex comparisons, followed by Tukey's post hoc test for elevated plus-maze test and open field test. Also, differences between groups were analyzed for statistical significance by using the unpaired t test. $P < 0.05$ was considered to be statistically significant.

Results

Abnormal behavior of transgenic mice

To determine aggressive behavior of male TgActβE mice, we performed the resident–intruder test. TgActβE mice showed anogenital contact and rearing at first, similar to that in wild-type mice. However, some TgActβE mice displayed aggressive behavior, i.e., offensive biting, sideways threat and tail rattling to the intruder mice (Table 1). These results suggested that TgActβE mice exhibited more response to the intruders than wild-type mice did. Since TgActβE16 mice showed similar phenotypes to TgActβE19 mice in the test, we hereinafter describe the behavioral abnormalities in TgActβE19 mice.

To further understand the abnormal emotion of TgActβE mice, we next performed the elevated plus-maze and open field tests. MANOVA revealed genotype differences in 13 dependent variables: total arm entries, percentage of total time and entries in the open and closed arms, and the frequency and total time of self grooming, rearing, stretching and peering [genotype: $F(13, 42) = 2.05$, $P < 0.05$]. TgActβE mice showed a significantly increased percentage of open arm entries [$F(1, 54) = 9.7$, $P < 0.01$] compared with that of wild-type mice, using bivariate analysis. TgActβE mice showed a significantly deceased percentage of closed arm entries [$F(1, 54) = 9.7$, $P < 0.01$] and total time spent in closed arms [$F(1, 54) = 7.33$, $P < 0.01$]. In addition, the total time and frequency of stress-evoked self grooming [time: $F(1, 54) = 4.08$, $P < 0.05$, frequency: $F(1, 54) = 7.76$, $P < 0.01$] were significantly increased in TgActβE mice. Univariate analysis by t test revealed that arm entries of male TgActβE mice were comparable with those of wild-type mice in the elevated plus-maze (Table 2). Furthermore, there was no significant difference in other parameters such as

Table 1
Resident–intruder test in male transgenic mice.

	Wild-type mice (%)	TgActβE mice (%)	Significance
Offensive biting	0.0	27.3	$P = 0.0624$
Sideways threat	0.0	54.5	$P < 0.01$
Tail rattling	0.0	9.1	$P = 0.3061$
Jumping	0.0	54.5	$P < 0.01$

Percentage of behavior elements is shown; $n = 11$.
χ^2 test was performed to determine differences between the groups.

Table 2
Behavioral analysis of transgenic mice on the elevated plus maze.

Genotype	Total arm entries	% Open arm entries	% Closed arm entries	% Time in open arms	% Time in closed arms	Stretching		Peering		Self grooming		Rearing	
						Time (%)	Frequency	Time (%)	Frequency	Time (%)	Frequency	Time (%)	Frequency
Male													
Wild-type	8.7 ± 1.4	9.3 ± 3.5	90.6 ± 3.5	8.1 ± 4.2	82.3 ± 4.8	2.1 ± 0.4	7.3 ± 1.1	1.0 ± 0.2	5.0 ± 0.9	4.5 ± 1.0	4.0 ± 0.7	4.1 ± 0.7	14.4 ± 2.2
TgActβE	9.6 ± 1.5	19.3 ± 4.9	80.7 ± 4.9	7.7 ± 2.4	72.5 ± 2.8	2.7 ± 0.5	9.5 ± 1.0	1.4 ± 0.4	7.4 ± 1.6	2.4 ± 0.4*	2.1 ± 0.3*	4.2 ± 0.7	13.0 ± 2.1
Female													
Wild-type	7.5 ± 1.2	20.5 ± 0.4	17.0 ± 5.0	17.0 ± 5.0	74.2 ± 5.0	3.2 ± 0.4	7.3 ± 0.7	2.1 ± 0.4	8.5 ± 1.4	5.6 ± 1.0	3.7 ± 0.5	5.4 ± 0.8	13.3 ± 1.7
TgActβE	6.6 ± 0.9	38.5 ± 5.9*	33.7 ± 8.5	33.7 ± 8.5	52.8 ± 8.1*	3.6 ± 1.0	7.4 ± 1.2	2.4 ± 0.4	10.8 ± 1.9	4.2 ± 0.8	2.6 ± 0.5	3.5 ± 0.7	8.8 ± 1.7

Values are mean ± SE. $n = 11–16$. *$P < 0.05$, compared with the wild-type mice of same sex.

stretching, peering from closed arms, and rearing. However, the total time and frequency of stress-evoked self grooming in closed arms were significantly decreased in male TgActβE mice (Table 2). On the other hand, in female TgActβE mice, the percentage of the open arm entries was significantly increased, and the percentage of closed arm entries and time spent in the closed arms were significantly decreased compared with those in wild-type mice (Table 2). The results indicated that female TgActβE mice had less anxiety than wild-type mice.

Furthermore, open field tests indicated that TgActβE mice had more exploratory behavior and less anxiety-like behavior than wild-type mice did (Supplementary data).

Decrease of c-Fos-positive cells in PVN and serum corticosterone level in TgActβE mice

Male and female TgActβE mice showed aggressive and anti-anxiety behavior, respectively. Therefore, we hypothesized that TgActβE mice have increased stress tolerance. To elucidate this hypothesis, the mice were exposed to restraint stress. Acute stress is known to evoke a discrete expression pattern of c-Fos, an inducer of neuronal activity, in the brain [11]. Corticotropin-releasing factor (CRF) is a central regulator of the hormonal stress response. It is thought that CRF-producing cells are abundant in the PVN [12,13]. c-Fos-expressing cells in transgenic hypothalamic PVN was detected by immunohistochemistry (Fig. 1A–D). c-Fos-positive cells were detected in the PVN of wild-type mice. However, the number of c-Fos-positive cells in the PVN of TgActβE mice was significantly decreased compared with that in wild-type mice (Fig. 1E). Consistently, serum corticosterone level after acute stress in TgActβE mice was lower than that in wild-type mice (Fig. 2). These results suggested that synthesis of CRF in response to stress was decreased in TgActβE mice.

Discussion

In the present study, we demonstrated that TgActβE mice exhibited abnormal behavior. Ectopic expression of activin E was detected in the transgenic choroid plexus of the brain (Supplementary data). It has been proposed that activin E is a negative regulator of cell growth. This concept has been supported by experiments in which overexpression of activin E in some types of cells has led to inhibition of cell growth in vivo and in vitro [3]. However, no prominent abnormalities, including apoptosis, were observed histologically in the transgenic brain. Furthermore, the relative weight of the brain to total body weight in the transgenic mice was comparable with that in wild-type mice (Supplementary data). These results indicated that ectopic expression of activin E in the brain caused the behavioral abnormalities. How does misexpressed activin E regulate the emotional behavior of TgActβE mice?

Ligands of the TGF-β superfamily exert their biological effects via a hetero-oligomeric complex of two types (type I and II) of transmembrane serine/threonine kinase receptors and Smads, which are intracellular receptor-associated proteins [14,15]. There are numerous combinations of ligand–receptor complexes that act as multiple TGF-β superfamily ligands. For example, activin receptors can bind activins, BMPs, Vg1, nodal, Lefty2 and GDF11. Based on similarities in the protein structure of activins, it is possible that activin E shares the receptors with other ligands.

Activin type I and II receptors are highly expressed in the forebrain [16,17]. It has been reported that activin A promotes neuron survival [18] and protects them from excitotoxic and ischemic damage [5]. A recent study by Agata et al. has shown that the transgenic mice with forebrain-specific expression of activin A (ACM4 mice) exhibit reduced anxiety in behavioral analysis [7]. The behavioral profiles of ACM4 mice resemble those of TgActβE mice. In female TgActβE mice, reduction of anxiety was also seen in elevated plus-maze tests and open field tests (Supplementary data). Therefore, activin E may mimic the activin A signal via the same receptor system and induce the behavior disorder in TgActβE mice. However, since ACM4 mice have enhanced locomotor activity that was not seen in TgActβE mice, the signal transduction of activin E may be slightly different from that of activin A. Further studies are needed to clarify the target cells and the signal transduction of activin E in the CNS.

Drosophila schnurri (Shn) and its vertebrate orthologs (shn-1, 2 and 3) are large zinc-finger-containing proteins [19,20]. Shn can interact with Smad proteins and regulate the signaling of TGF-β superfamily members [21]. Shn-2-deficient mice (Shn-$2^{-/-}$ mice) show hypersensitivity to stress, accompanied by anxiety-like behavior [10]. The sensitivity to anxiety of TgActβE mice was opposite to the phenotype of Shn-$2^{-/-}$ mice, therefore, Shn-2 may transduce the activin E signal that regulates the CNS.

The stress response is thought to be mediated by CRF, which is known to be a regulator of the hypothalamic–pituitary–adrenal (HPA) axis [22]. Alterations in the HPA axis have been related to various behavioral responses, including aggression and anxiety. c-Fos expression is considered to be one of the markers of brain activity, and its induction is often used to evaluate stress-related responses because it can be triggered by various stressors [11]. The stress-induced c-Fos expression in PVN cells in TgActβE mice was lower than that in wild-type mice. Furthermore, TgActβE mice showed stimulated aggressive behavior in the resident–intruder test and less anxiety-like behavior in the elevated plus-maze and open field tests. Taken together, these results suggest that activin E may act as a regulator of the HPA axis. However, it is known that activation of the HPA axis is correlated positively with anxiety and aggressive behavior [13,23]. These observations are not consistent with the data from TgActβE mice. Although the concentration of serum corticosterone in female TgActβE mice after acute stress

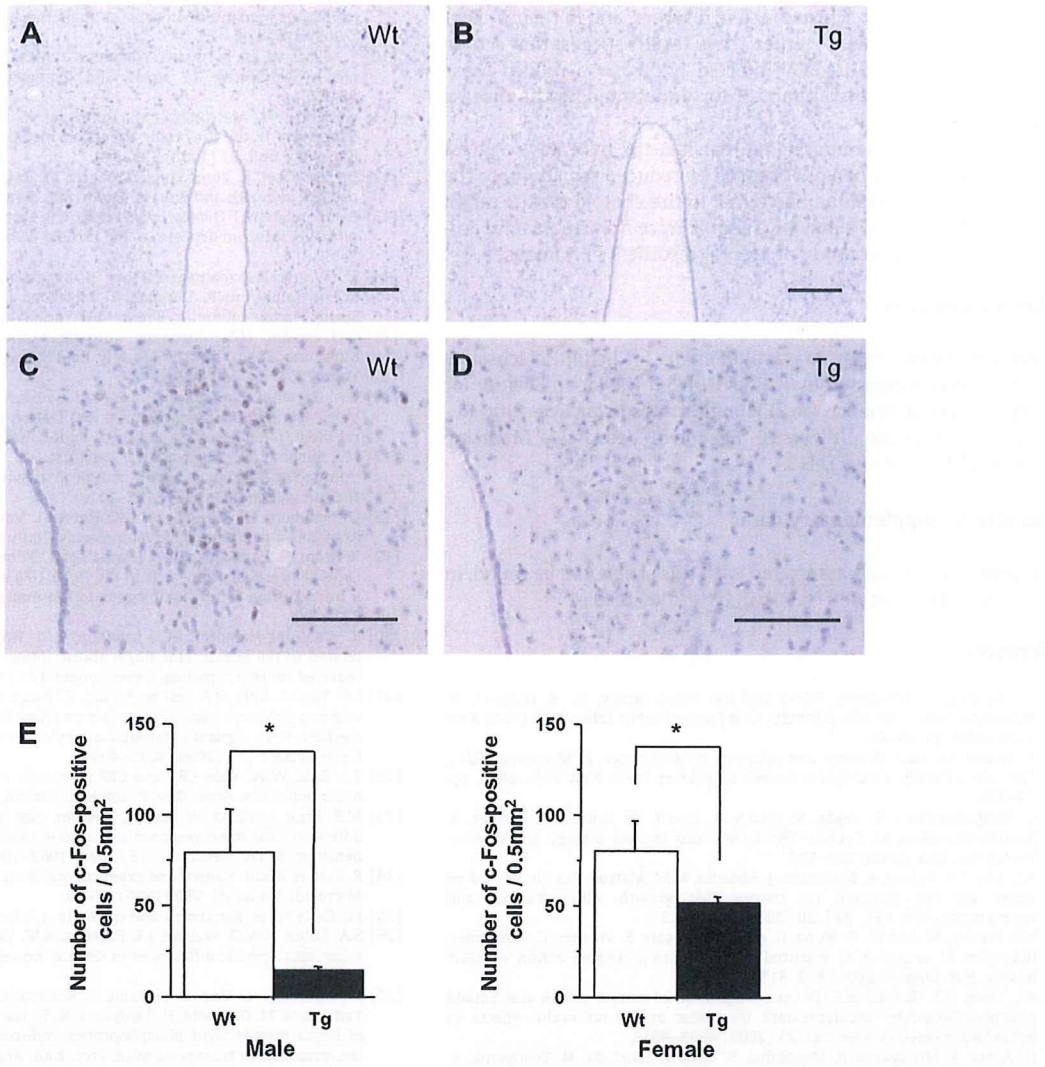

Fig. 1. c-Fos-positive cells in the PVN of TgActβE mice. Section from the mice subjected to restraint prior to sacrifice were immunoreacted for c-Fos. Photograph of male wild-type (A,C) and TgActβE (B,D) mice. Bar, 100 μm. Representative data are shown. The number of c-Fos-positive cells in the PVN was counted in one representative section (0.5 mm^2) from each mouse, and the mean for the male and female mice is shown (E). Values are means ± SE. $n = 4$–5. $^{*}P < 0.05$.

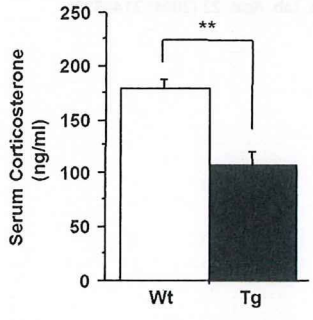

Fig. 2. Serum corticosterone level in TgActβE mice. Serum corticosterone concentration was determined after 30 min restraint stress in 14-week-old male TgActβE mice. Wt, wild-type mouse; Tg, TgActβE mice. Values are means ± SE. $n = 4$. $^{**}P < 0.01$.

was lower than that in wild-type mice, it was not statistically significant (Date not shown). Furthermore, the elevated plus-maze test revealed that the genotype differences in the behavior of TgActβE mice. Therefore, the abnormality in not only stress response but also other system might underlie the abnormal behaviors in the transgenic mice. Further analysis of the effect of activin E on the CNS is required to clarify the behavioral abnormalities in the transgenic mice.

The question arises as to what the behavioral abnormality induced by misexpression of activin E represents pathophysiologically. Recently, Nishino et al. have reported the involvement of the TGF-β superfamily, especially activin E, in neuronal disorders of rats infected with BDV [8]. Gene expression for the activin βE subunit in the rat brain is up-regulated by BDV infection. BDV is a neurotropic and single-stranded enveloped RNA virus that persistently infects the CNS of various animals and may cause behavioral abnormalities [24,25]. Experimental BDV infection in rodents also induces behavioral and neurological disturbances that resemble those in psychiatric patients, including those with autism, schizophrenia or mood disorders [26,27]. Interestingly, BDV genomic transcripts have been detected in neuropsychiatric patients [28]. Furthermore, viral RNA from BDV has been detected in patients

with schizophrenia or schizoaffective disorder, and in their biological relatives [29]. Taken together, these results suggest that activin βE subunit expressed in BDV-infected brain has a role in these mental disorders and is important for understanding the disease pathophysiologically.

In summary, we demonstrated that TgActβE mice have aggressive and low-anxiety behavior caused by reduced sensitivity to the stress. Ectopic expression of activin E in the choroid plexus might influence the CNS and behavior. TgActβE mice may be a useful animal model for further study of mental disorders in humans.

Acknowledgments

We are grateful to Dr. Masayuki Funaba for helpful discussion. This work was supported by KAKENHI from the Japan Society for the Promotion of Science (to O.H.) and a Grant for Scientific Research from Kitasato University, School of Veterinary Medicine and Animal Sciences (to O.H.).

Appendix A. Supplementary data

Supplementary data associated with this article can be found, in the online version, at doi:10.1016/j.bbrc.2009.05.054.

References

[1] R. Derynck, K. Miyazono, TGF-β and the TGF-β family, in: R. Derynck, K. Miyazono (Eds.), The TGF-β Family, Cold Spring Harbor Laboratory Press, New York, 2008, pp. 29–43.
[2] E. Wiater, W. Vale, Activins and inhibins, in: R. Derynck, K. Miyazono (Eds.), The TGF-β Family, Cold Spring Harbor Laboratory Press, New York, 2008, pp. 79–120.
[3] C. Rodgarkia-Dara, S. Vejda, N. Erlach, A. Losert, W. Brusch, W. Berger, R. Schulte-Hermann, M. Grusch, The activin axis in liver biology and disease, Mutat. Res. 613 (2006) 123–137.
[4] A.L. Lau, T.R. Kumar, K. Nishimori, J. Bonadio, M.M. Matzuk, Activin βC and βE genes are not essential for mouse liver growth, differentiation, and regeneration, Mol. Cell. Biol. 20 (2000) 6127–6137.
[5] Y.P. Tretter, M. Hertel, B. Munz, G. ten Bruggencate, S. Werner, C. Alzheimer, Induction of activin A is essential for the neuroprotective action of bFGF in vivo, Nat. Med. 6 (2000) 812–815.
[6] A.L. Dow, D.S. Russell, R.S. Duman, Regulation of activin mRNA and Smad2 phosphorylation by antidepressant treatment in the rat brain: effects in behavioral models, J. Neurosci. 25 (2005) 4908–4916.
[7] H. Ageta, A. Murayama, R. Migishima, S. Kida, K. Tsuchida, M. Yokoyama, K. Inokuchi, Activin in the brain modulates anxiety-related behavior and adult neurogenesis, PLoS ONE 3 (2008) e1869.
[8] Y. Nishino, R. Ooishi, S. Kurokawa, K. Fujino, M. Murakami, H. Madarame, O. Hashimoto, K.M. Carbone, M. Funaba, Gene expression of the TGF-β family in rat brain infected with Borna disease virus, Microbes Infect., 2009, doi:10.1016/j.micinf.2009.04.014.
[9] O. Hashimoto, Y. Ushiro, K. Sekiyama, O. Yamaguchi, K. Yoshioka, K. Mutoh, Y. Hasegawa, Impaired growth of pancreatic exocrine cells in transgenic mice expressing human activin betaE subunit, Biochem. Biophys. Res. Commun. 341 (2006) 416–424.
[10] T. Takagi, W. Jin, K. Taya, G. Watanabe, K. Mori, S. Ishii, Schnurri-2 mutant mice are hypersensitive to stress and hyperactive, Brain Res. 1108 (2006) 88–97.
[11] E. Senba, K. Matsunaga, M. Tohyama, K. Noguchi, Stress-induced c-fos expression in the rat brain: activation mechanism of sympathetic pathway, Brain Res. Bull. 31 (1993) 329–344.
[12] E.R. De Kloet, E. Vreugdenhil, M. Oitzl, M. Joels, Brain corticosteroid receptor balance in health and disease, Endocrinol. Rev. 19 (1998) 269–301.
[13] L. Arborelius, M.J. Owens, P.M. Plotsky, C.B. Nemeroff, The role of corticotropin-releasing factor in depression and anxiety disorders, J. Endocrinol. 160 (1999) 1–12.
[14] J.L. Wrana, B. Ozdamar, LeC Roy, H. Benchabane, Signaling receptors of the TGF-β family, in: R. Derynck, K. Miyazono (Eds.), The TGF-β Family, Cold Spring Harbor Laboratory Press, New York, 2008, pp. 151–177.
[15] C-H. Heldin, TGF-β signaling from receptors to smads, in: R. Derynck, K. Miyazono (Eds.), The TGF-β Family, Cold Spring Harbor Laboratory Press, New York, 2008, pp. 259–285.
[16] V.A. Cameron, E. Nishimura, L.S. Mathews, K.A. Lewis, P.E. Sawchenko, W.W. Vale, Hybridization histochemical localization of activin receptor subtypes in rat brain, pituitary ovary and testis Endocrinol. 134 (1994) 799–808.
[17] M. Funaba, T. Murata, H. Fujimura, E. Murata, M. Abe, K. Torii, Immunolocalization of type I or type II activin receptors in the rat brain, J. Neuroendocrinol. 9 (1997) 105–111.
[18] D. Schubert, H. Kimura, M. LaCorbiere, J. Vaughan, D. Karr, W.H. Fischer, Activin is a nerve cell survival molecule, Nature 344 (1990) 868–870.
[19] K. Arora, H. Dai, S.G. Kazuko, J. Jamal, M.B. O'Connor, A. Letsou, R. Warrior, The *Drosophila schnurri* gene acts in the Dpp/TGFβ signaling pathway and encodes a transcription factor homologous to the human MBP family, Cell 81 (1995) 781–790.
[20] K. Staehling-Hampton, A.S. Laughon, F.M. Hoffmann, A *Drosophila* protein related to the human zinc finger transcription factor, PRDII/MBPI/HIV-EP1 is required for dpp signaling, Development 121 (1995) 3393–3403.
[21] L.C. Yao, I.L. Blitz, D.A. Peiffer, S. Phin, Y. Wang, S. Ogata, K.W. Cho, K. Arora, R. Warrior, Schnurri transcription factors from *Drosophila* and vertebrates can mediate Bmp signaling through a phylogenetically conserved mechanism, Development 133 (2006) 4025–4034.
[22] T.L. Bale, W.W. Vale, CRF and CRF receptors: role in stress responsivity and other behaviors, Annu. Rev. Pharmacol. Toxicol. 44 (2004) 525–557.
[23] M.R. Kruk, J. Halász, W. Meelis, J. Haller, Fast positive feedback between the adrenocortical stress response and a brain mechanism involved in aggressive behavior, Behav. Neurosci. 118 (2004) 1062–1070.
[24] R. Rott, H. Becht, Natural and experimental Borna disease in animals, Curr. Top. Microbiol. Immunol. 190 (1995) 17–30.
[25] J.C. De la Torre, Bornavirus and the brain, J. Infect. Dis. 186 (2002) S241–S247.
[26] S.A. Rubin, R.W.D. Waltrip, J.R. Bautista, K.M. Carbone, Borna disease virus in mice: host-specific differences in disease expression, J. Virol. 67 (1993) 548–552.
[27] W. Kamitani, E. Ono, S. Yoshino, T. Kobayashi, S. Taharaguchi, B.J. Lee, M. Yamashita, M. Okamoto, H. Taniyama, K. Tomonaga, K. Ikuta, Glial expression of Borna disease virus phosphoprotein induces behavioral and neurological abnormalities in transgenic mice, Proc. Natl. Acad. Sci. USA 100 (2003) 8969–8974.
[28] L. Bode, W. Zimmermann, R. Ferszt, F. Steinbach, H. Ludwig, Borna disease virus genome transcribed and expressed in psychiatric patients, Nat. Med. 1 (1995) 232–236.
[29] S.O. Nunes, E.N. Itano, M.K. Amarante, E.M. Reiche, H.C. Miranda, C.E. de Oliveira, T. Matsuo, H.O. Vargas, M.A. Watanabe, RNA from Borna disease virus in patients with schizophrenia, schizoaffective patients, and in their biological relatives, J. Clin. Lab. Anal. 22 (2008) 314–320.

STEM CELLS®
TISSUE-SPECIFIC STEM CELLS

Astrocyte Differentiation of Neural Precursor Cells is Enhanced by Retinoic Acid Through a Change in Epigenetic Modification

HIROTSUGU ASANO, MAKOTO AONUMA, TSUKASA SANOSAKA, JUN KOHYAMA, MASAKAZU NAMIHIRA, KINICHI NAKASHIMA

Laboratory of Molecular Neuroscience, Graduate School of Biological Sciences, Nara Institute of Science and Technology, Ikoma, Nara, Japan

Key Words. Retinoic acid • Neural precursor cells • STAT3 • Astrocyte • Histone acetylation

ABSTRACT

Neurons, astrocytes, and oligodendrocytes—the three major cell types that comprise the central nervous system—are generated from common multipotent neural precursor cells (NPCs). Members of the interleukin-6 family of cytokines, including leukemia inhibitory factor (LIF), induce astrocyte differentiation of NPCs by activating the transcription factor signal transducer and activator of transcription 3 (STAT3). We show here that retinoic acid (RA) facilitates LIF-induced astrocyte differentiation of NPCs. RA and LIF synergistically activate the promoter of *gfap*, which encodes the astrocytic marker glial fibrillary acidic protein, and a putative RA response element in the promoter was found to be critical for this activation. Histone H3 acetylation around the STAT-binding site in the *gfap* promoter was increased in NPCs treated with RA, allowing STAT3 to gain access to the promoter more efficiently. These results suggest that RA acts in concert with LIF to induce astrocyte differentiation of NPCs through an epigenetic mechanism that involves cross-talk between distinct signaling pathways. Stem Cells *2009;27:2744–2752*

Disclosure of potential conflicts of interest is found at the end of this article.

INTRODUCTION

Multipotent neural precursor cells (NPCs) are defined as cells that can self-renew and give rise to the three major cell types in the central nervous system (CNS): neurons, astrocytes, and oligodendrocytes. However, NPCs lack multipotentiality in early gestation, and differentiate only into neurons at mid-gestation. NPCs later acquire multipotentiality and start to differentiate into astrocytes and oligodendrocytes during late gestation [1, 2]. This sequential differentiation of NPCs appears to be temporally and spatially regulated by both cell-external cues, including cytokine signaling, and cell-internal programs such as epigenetic modification [3–6].

The interleukin (IL)-6 family of cytokines share membrane glycoprotein gp130 as a critical receptor component for activation of the downstream janus kinase (JAK)-signal transducer and activator of transcription (STAT) pathway, and have been shown to induce astrocyte differentiation of NPCs [7–9]. One member of this family, leukemia inhibitory factor (LIF), signals through its heterodimeric receptor complex, which is composed of LIF receptor (LIFR)-β and gp130. Gene knockouts of LIF, LIFRβ, gp130, and STAT3 all result in impaired astrocyte differentiation in vivo, further indicating that JAK-STAT signaling contributes to astrogliogenesis in the developing CNS [8, 10–12]. Bone morphogenetic proteins (BMPs) also contribute to the expression of astrocyte-specific genes via complex formation between the BMP-downstream transcription factor Smad1 and STATs, bridged by the transcription coactivator p300/CREB-binding protein (CBP) [13, 14].

Epigenetic modifications include both DNA methylation and histone modifications such as acetylation, methylation, phosphorylation, and ubiquitinylation [15, 16]. We have previously shown that a CpG dinucleotide within the STAT3 recognition sequence in the astrocytic marker glial fibrillary acidic protein (*gfap*) gene promoter is highly methylated in NPCs at mid-gestation, when the cells have not yet acquired the potential to differentiate into astrocytes [4]. Since STAT3 is unable to bind to the methylated cognate recognition sequence [4, 17], midgestational NPCs cannot express *gfap* even when they are stimulated by astrocyte-inducing cytokines such as LIF. As gestation proceeds, however, the STAT3-binding site becomes demethylated in NPCs, enabling the cells to express *gfap* in response to LIF stimulation. Based on these findings, we have suggested that DNA methylation is a critical cell-intrinsic determinant of astrocyte differentiation during brain development [4, 6].

Histone acetylation, mediated by transcriptional coactivators having histone acetyltransferase (HAT) activity such as p300/CBP, has been shown to correlate with gene activation [15, 16]. Conversely, gene repression is associated with histone deacetylation, which favors chromatin condensation. Transcriptional repressors, such as nuclear receptor corepressor (N-CoR) and neuron-restrictive silencer factor/repressor element-1 silencing transcription factor (NRSF/REST), have

Author contributions: H.A., J.K., M.N., K.N.: designed research; H.A., M.A., T.S.: performed research; H.A., M.N., K.N.: analyzed data; H.A., M.N., K.N.: wrote the manuscript; K.N., financial support.

Correspondence: Kinichi Nakashima, Ph.D., Laboratory of Molecular Neuroscience, Graduate School of Biological Sciences, Nara Institute of Science and Technology, 8916-5, Takayama, Ikoma, Nara 630-0192, Japan. Telephone: +81-743-72-5471; Fax: +81-743-72-5479; e-mail: kin@bs.naist.jp Received February 17, 2009; accepted for publication July 2, 2009; first published online in STEM CELLS *EXPRESS* Month 00, 2009. 1066-5099/2009/$30.00/0 doi: 10.1002/stem.176

been found in complexes with histone deacetylases (HDACs) on gene regulatory regions [18, 19].

Retinoid acid (RA) acts through RA receptors (RARs), which are members of the nuclear receptor superfamily. RARs bind, together with their heterodimeric partners the retinoid X receptors (RXRs), to RA response elements (RAREs) in the promoter regions of target. In the absence of RA ligand, RARs associate with either N-CoR or silencing mediator of retinoic acid and thyroid hormone receptors (SMRT), leading to repression of target genes by recruitment of HDACs [20–24]. When RA binds to its cognate receptor, however, HDACs are released from the RAR-RXR heterodimer and transcriptional coactivators with HAT activity are instead recruited [20–23]. In addition, it has recently been reported that many HDAC-regulated genes are also targeted by RAR [25].

Expression of RA-synthesizing and -degrading enzymes and of RARs has been shown in the developing brain [26–31]. In transgenic mice carrying a reporter gene for RA signal activation, RA signaling is shown to be indeed active in embryonic brain [31–33], and gene knockouts of RA-synthesizing and -degrading enzymes and of RARs yield impaired development of the CNS [27, 30, 34–38]. Thus, it is reasonable to hypothesize that RA signaling may be involved in the fate specification of NPCs during development. Furthermore, although RA has indeed been shown to induce neuronal differentiation of NPCs [24, 39], the extent to which it participates in differentiation into other lineages remains to be fully elucidated.

Although histone acetylation has been shown to correlates with gene activation, its precise molecular mechanisms are not fully understood. In this study, we show that RA acts synergistically with LIF to induce astrocyte differentiation of NPCs. Synergistic activation of the *gfap* promoter was virtually abolished by either deletion or mutation of a putative RARE in the promoter. We also found that RA stimulation of NPCs facilitates STAT3 binding to the *gfap* promoter, probably through the relaxation of chromatin caused by RA-induced histone acetylation around the STAT3-binding site. Furthermore, as in the case of RA stimulation, treatment with the HDAC inhibitor valproic acid (VPA) increased histone acetylation in NPCs, leading to enhanced STAT3 binding to the *gfap* promoter. Our results therefore suggest that RA-induced histone acetylation participates in astrocyte differentiation of NPCs by facilitating STAT3 binding to an astrocyte-specific gene promoter.

Materials and Methods

NPC Culture

Pregnant ICR mice were used to prepare NPCs. The experimental protocols described below were performed according to the animal experimentation guidelines of Nara Institute of Science and Technology. NPCs were prepared from telencephalons of E14.5 mice and cultured as described previously [4, 13]. Briefly, the telencephalons were triturated in Hank's balanced salt solution (HBSS) by mild pipetting with a 1-ml pipet tip. Dissociated cells were cultured for 4 days in N2-supplemented Dulbecco's modified Eagle's medium (DMEM) with F12 containing 10 ng/ml basic FGF (N2/DMEM/F12/bFGF; R&D Systems Inc., Minneapolis, http://www.rndsystems.com) on culture dishes which had been precoated with poly-L-ornithine and fibronectin (Sigma-Aldrich, St. Louis, http://www.sigmaaldrich.com). Cells were detached in HBSS and replated onto chamber slides, 60-mm culture dishes, or 12-well plates (Nunc, Rochester, NY, http://www.nuncbrand.com), precoated as above, and cultured in N2/DMEM/F12/bFGF. RA (1 μM, Sigma), LIF (50 ng/ml, Chemicon, Temecula, CA, http://www.chemicon.com) and VPA (1 mM, Sigma) were added singly or in combination, as appropriate, to examine their effects on differentiation of NPCs. Cells cultured on coated chamber slides were washed with PBS, fixed in 4% paraformaldehyde in PBS, and stained with anti-GFAP antibody (DAKO, Glostrup, Denmark, http://www.dako.com) and Cy3-conjugated second antibody (Jackson Immunoresearch Laboratories, West Grove, PA, http://www.jacksonimmuno.com). Nuclei were stained using bisbenzimide H33258 fluorochrome trihydrochloride (Nacalai Tesque, Kyoto, Japan, www.nacalai.co.jp/en). Stained cells were visualized with fluorescence microscope (Axiovert 200M, Carl Zeiss, Jena, Germany, http://www.zeiss.com).

Reverse-Transcription Polymerase Chain Reaction

Total RNA was isolated from NPCs that had been cultured with LIF for 8 hours in the presence or absence of RA. Reverse transcription was performed with SuperScript II reverse transcriptase (Invitrogen, Carlsbad, CA, http://www.invitrogen.com) and polymerase chain reaction (PCR) reactions were performed using Amplitaq Gold (Applied BioSystems, Foster City, CA, http://www.appliedbiosystems.com). The following primers were used: *gfap*: GFAP-S, 5′-CACGAACGAGTCCCTAGAGC-3′, and GFAP-AS, 5′-TCACATCACCACGTCCTTG-3′; *g3pdh*: G3PDH-S, 5′- ACCACAGTCCATGCCATCAC-3′, and G3PDH-AS, 5′-TCCACCACCCTGTTGCTGT A-3′.

Promoter Assay

NPCs cultured for 4 days on 10-cm dishes as described above were replated onto 12-well plates (Nunc) and transfected the next day with a plasmid containing the firefly luciferase gene under the regulation of the 2.5-kb *gfap* promoter (GF1L) [13], the 1.9-kb *gfap* promoter (GF1LB, Fig. 3A) [13], or with a modified construct in which nucleotide substitutions were introduced into the GF1L sequences 5′-TTCCGAGAA-3′, a STAT3-binding site (GF1L-SBSPM) [4], or 5′-AGTTCAAGGTCA-3′, a putative RARE (GF1L-RAREPM, Fig. 3B). As an internal control, the sea pansy luciferase gene conjugated with human elongation factor-1α promoter (R-Luc) was also cotransfected [13]. Transfection was performed using Trans-IT LT1 (Mirus Bio, Madison, WI, www.mirusbio.com) according to the manufacturer's procedures. On the day after transfection, cells were stimulated with LIF (50 ng/ml) and/or RA (1 μM) for 8 hours and then solubilized. Luciferase activity was measured according to the procedures recommended for the Dual Luciferase Reporter Assay System (Promega, Madison, WI, http://www.promega.com), using Wallac 1,420 ARVO/Light (PerkinElmer Life and Analytical Sciences, Boston, MA, http://www.perkinelmer.com) luminometer was used for detection. Firefly luciferase activity was divided by sea pansy luciferase activity from the cotransfected control plasmid, R-Luc.

Chromatin Immunoprecipitation Assay

Chromatin immunoprecipitation was performed according to a protocol published by Upstate Biotechnology (Charlottesville, VA, http://www.upstate.com), with minor modifications. Cells were exposed to formaldehyde at a final concentration of 1%, added directly to the tissue culture medium. The cells were centrifuged to a pellet after 10 min of formaldehyde exposure, lysed in lysis buffer (1% SDS, 10 mM EDTA, 50 mM Tris-HCl [pH 8.1]) containing a protease inhibitor cocktail (Nacalai Tesque), and then incubated for 10 min on ice. Cell lysates were sonicated using a microtip (Branson Ultrasonics, Danbury, CT, www.bransonultrasonics.com) until the DNA fragments were 500–1,000 base pairs in length. These chromatin samples were diluted 1:10 with dilution buffer (1.1% Triton X-100, 0.11% NaDOC, 50 mM Tris-HCl [pH 8.1], 167 mM NaCl), and 2.5% of the total volume was stored as input at −20°C until use. Immunoprecipitation was performed at 4°C overnight with 2 μg of an antibody against STAT3, RARα, RARβ, RXR (Santa Cruz Biotechnology Inc., Santa Cruz, CA, http://www.scbt.com) or acetylated histone H3 (Upstate Biotechnology) after the samples were precleared with salmon sperm DNA/protein A agarose (Upstate Biotechnology).

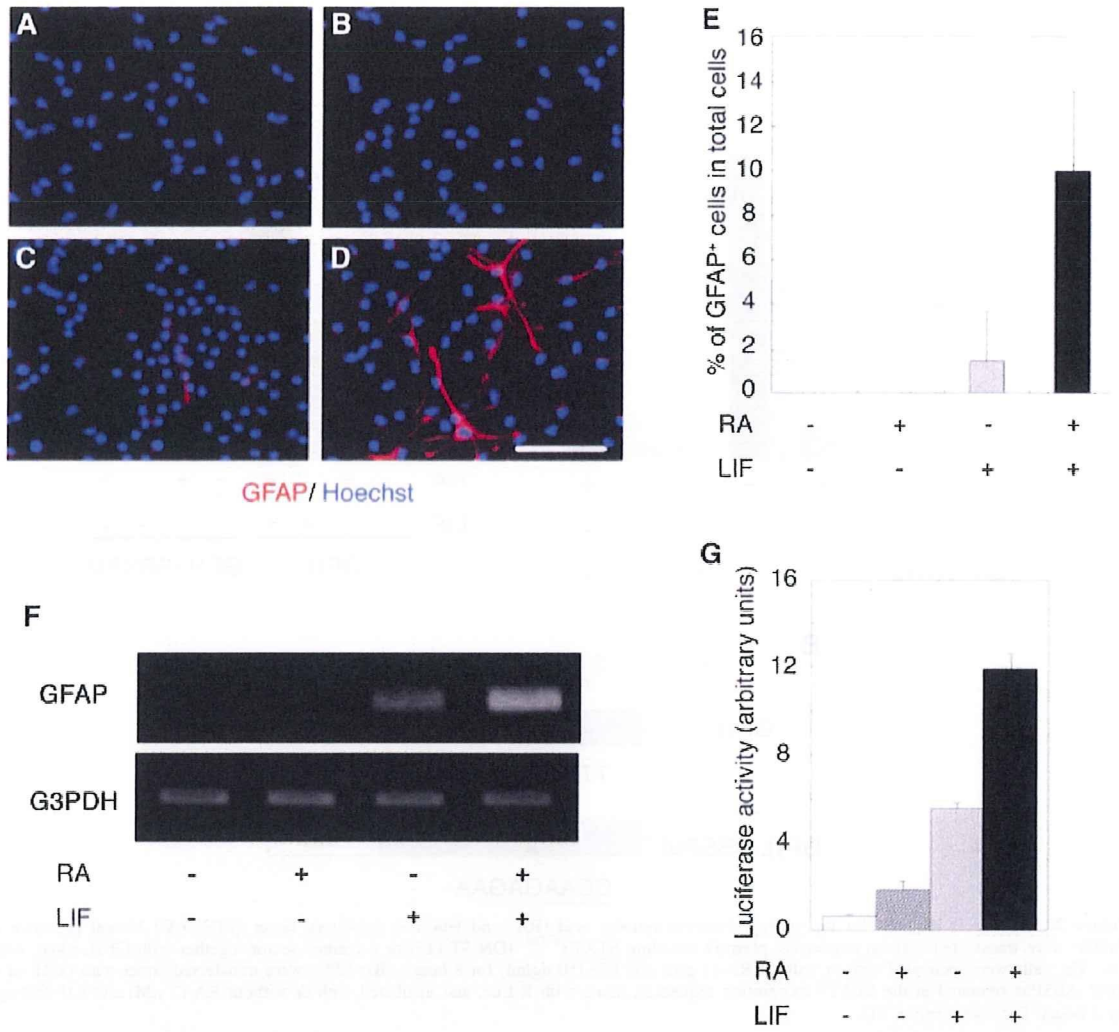

Figure 1. Synergistic induction of astrocyte differentiation of neural precursor cells (NPCs) by retinoic acid (RA) and leukemia inhibitory factor (LIF). NPCs were cultured with medium alone **(A)**, RA (1 μM) **(B)**, LIF (50 ng/ml) **(C)**, or RA (1 μM) plus LIF (50 ng/ml) **(D)** for 2 days. The cells were then stained with antibody against glial fibrillary acidic protein (GFAP; red) and with Hoechst 33258 (blue). Scale bar = 50 μm. **(E):** Percentage of GFAP-positive cells in total cells was calculated. **(F):** Total RNA was extracted from NPCs cultured as above with medium alone, RA, LIF, or RA plus LIF, and was analyzed by reverse-transcription polymerase chain reaction using specific primers for *gfap* and *g3pdh*. **(G):** *gfap* promoter assays were performed for cells transfected with a firefly luciferase gene reporter construct containing the 2.5-kb mouse *gfap* promoter (GF1L) along with R-Luc, following incubation with or without RA and/or LIF for 8 hours. Data in graphs are mean ± SD.

Immune complexes were collected by salmon sperm DNA/protein A agarose and washed successively with the following buffers: low-salt buffer (0.1% SDS, 1% Triton X-100, 0.1% NaDOC, 1 mM EDTA, 50 mM Tris-HCl [pH 8.1], 167 mM NaCl), high-salt buffer (0.1% SDS, 1% Triton X-100, 0.1% NaDOC, 1 mM EDTA, 50 mM Tris-HCl [pH 8.1], 500 mM NaCl), LiCl buffer (0.25 M LiCl, 0.5% NP-40, 0.5% NaDOC, 1 mM EDTA, 10 mM Tris-HCl [pH 8.1]), and TE buffer (10 mM Tris-HCl, 1 mM EDTA [pH 8.0]). Immune complexes were disrupted with direct elution buffer (0.5% SDS, 5 mM EDTA, 10 mM Tris-HCl [pH 8.1], 300 mM NaCl) and the covalent links between immunoprecipitates and input chromatin were disrupted by incubation with 300 mM NaCl at 65°C for 4 hours or overnight. DNA was further incubated with RNase and proteinase K (Nacalai Tesque), purified by phenol extraction, and ethanol precipitated. DNA pellets were dissolved in 20 μl of H_2O and used as a template for PCR or quantitative PCR (qPCR). The following sets of primers were used: GSS (5′-TAAGCTGAAGACCTGGCAGTG-3′) and GSAS (5′-TGCTGAATAGAGCCTTGTTCTC-3′) for PCR, GSSQ (5′-TGACTCACCTTGGCATAGACAT-3′) and GSASQ (5′-CTGCTTTTATCCCAGGATGC-3′) for qPCR of the STAT3-binding site-containing region of the *gfap* promoter, GF-RARE-S (5′-CACAGGAGGTGTGGTGGCTA-3′) and GF-RARE-AS (5′-GGTTTGTCAGCAACGCTGGA-3′) for PCR, GF-RARE-SQ (5′-GCTTAAGGCTGGAAGACACAG -3′) and GF-RARE-ASQ, (5′-CTGGATCTAGGACTTGCTTCGT-3′) for qPCR of the RARE-containing region of the *gfap* promoter.

Results

RA and LIF Synergistically Induce Astrocyte Differentiation of NPCs

As a first step toward testing the possibility that RA signaling plays a role in fate specification of NPCs, we examined the

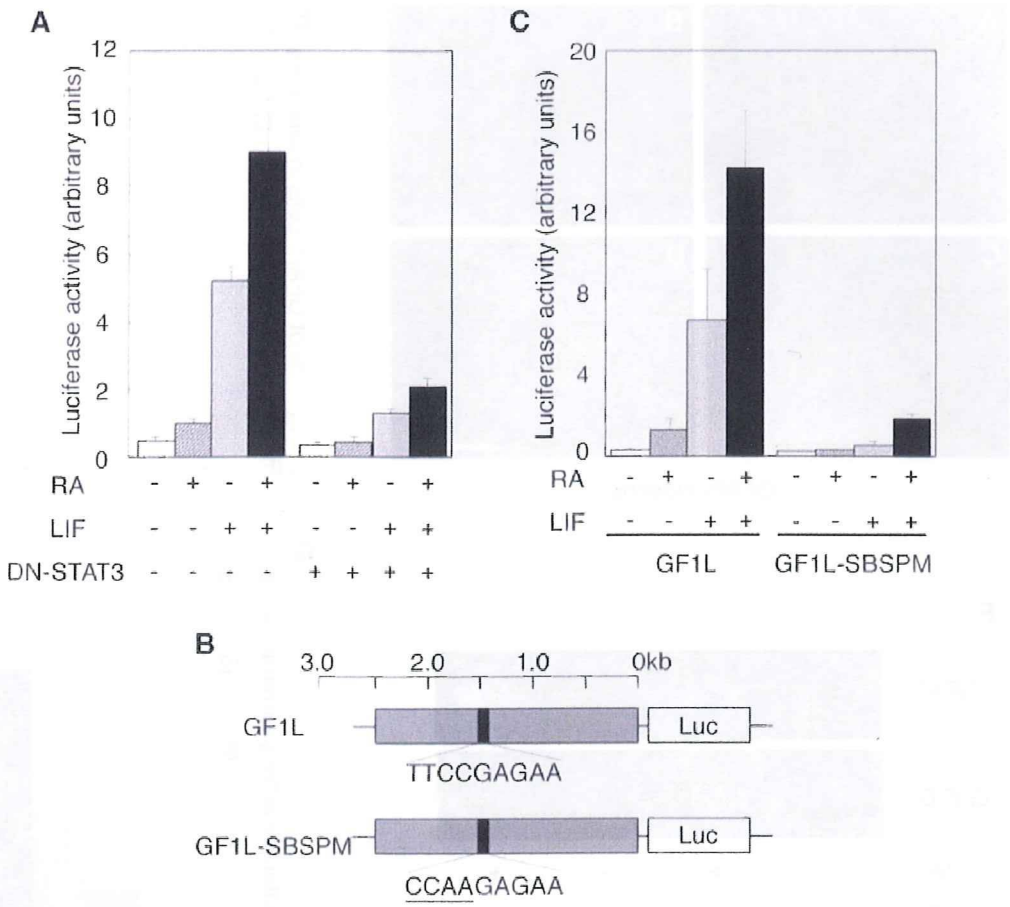

Figure 2. STAT3 is required for the synergy between retinoic acid (RA) and leukemia inhibitory factor (LIF). **(A):** Neural precursor cells (NPCs) were transfected with an expression plasmid encoding $STAT3^{Y705F}$ (DN-STAT3) or a control vector together with GF1L along with R-Luc. The cells were incubated with or without RA (1 μM) and LIF (50 ng/ml) for 8 hours. **(B):** NPCs were transfected either with GF1L or with GF1L-SBSPM (mutated in the STAT3 recognition sequence), along with R-Luc, and incubated with or without RA (1 μM) and LIF (50 ng/ml) for 8 hours. Data are mean ± SD.

expression of RAR and RXR family genes in NPCs and found that they were indeed expressed (supporting information Fig. 1). We next investigated the effect of RA on astrocyte differentiation of NPCs. NPCs prepared from E14.5 mouse telencephalons were cultured for 2 days with RA, with LIF, with RA together with LIF, or left untreated. The cells were then stained with an antibody against the astrocyte-specific marker GFAP. As shown in Figure 1, a small number of GFAP-positive astrocytes were induced in the presence of LIF, whereas RA alone induced no GFAP-positive cells (Fig. 1A–C, 1E). However, GFAP-positive astrocyte differentiation was induced synergistically when the NPCs were treated simultaneously with RA and LIF (Fig. 1D, 1E). We also examined another astrocytic marker, S100β, whose expression begins earlier than that of GFAP in the course of astrocytic differentiation [40]. In contrast to the case of GFAP, RA alone induced S100β–positive cells in NPCs (supporting information Fig. 2). This is probably because that S100β is an earlier marker for astrocyte differentiation than GFAP [40]. Therefore, this gene has already become competent to be induced by either RA or LIF alone by this developmental stage, although the precise mechanism is currently unknown.

To unravel the mechanism whereby RA and LIF synergistically induce GFAP-positive astrocyte differentiation of NPCs, we next performed RT-PCR analysis. *gfap* mRNA increased markedly in the costimulated condition with RA and LIF compared to treatments with LIF or RA alone (Fig. 1F), indicating that RA acts at the transcriptional level to enhance LIF-induced GFAP-positive astrocyte differentiation.

Given that RA affects *gfap* expression, we carried out a reporter assay using the *gfap* promoter construct GF1L-pGL3 [4, 13]. As shown in Figure 1G, although the *gfap* promoter was barely activated by RA alone, synergistic activation was observed when the NPCs were treated with RA and LIF simultaneously. These results indicate that RA and LIF synergistically induce astrocyte differentiation of NPCs.

STAT3 Is Essential for Synergistic Activation of the *Gfap* Promoter by RA and LIF

STAT3 plays a critical role as a downstream molecule in IL-6 family cytokine-signaling pathways [4, 7, 8, 13]. Therefore, to investigate whether STAT3 is also essential for synergistic activation of the *gfap* promoter by RA and LIF, we performed

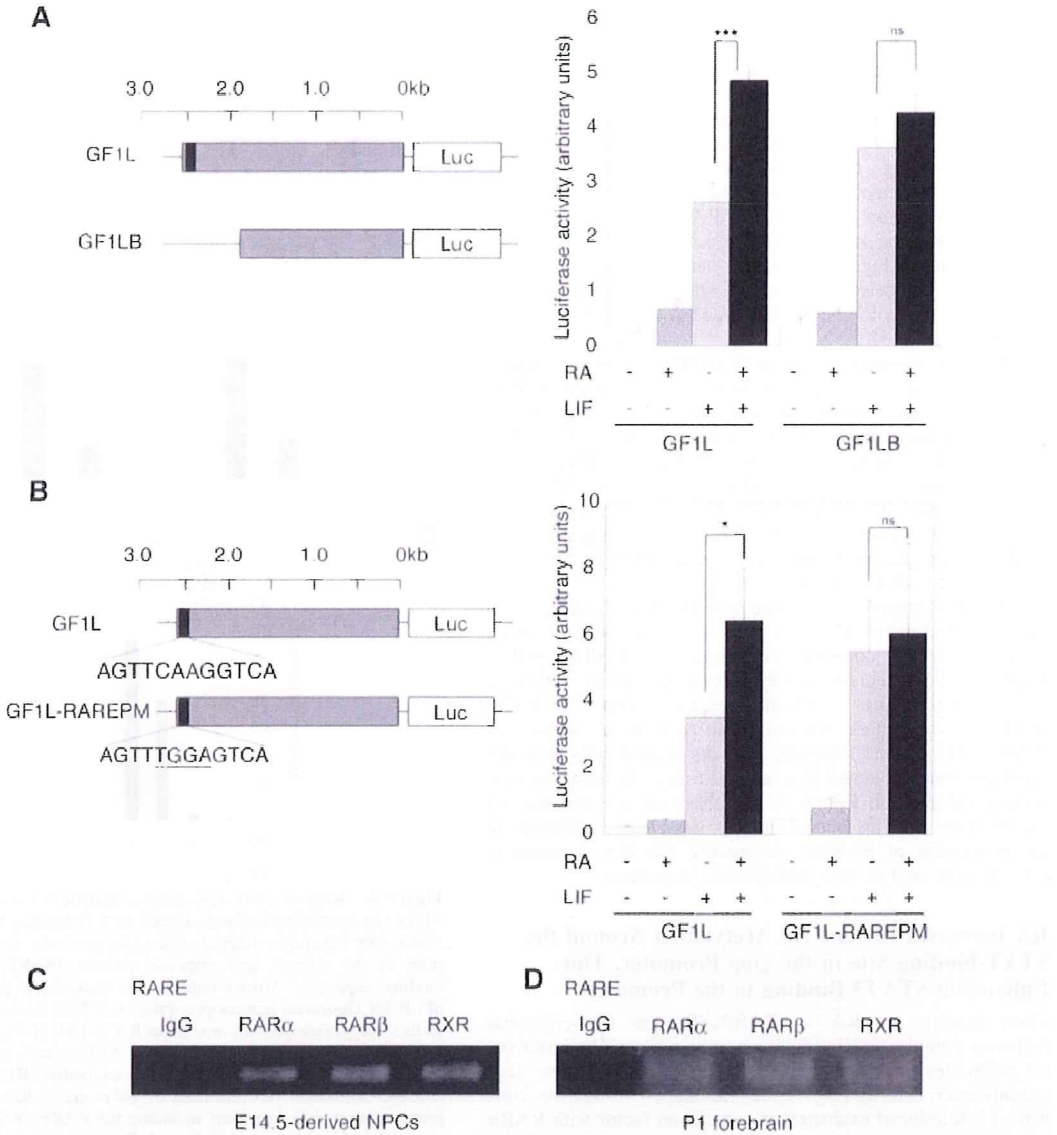

Figure 3. A retinoic acid response element (RARE) in the *gfap* promoter is essential for the synergistic activation by retinoic acid (RA) and leukemia inhibitory factor (LIF). Neural precursor cells (NPCs) were transfected with either GF1L or GF1LB (**A**), or GF1L-RAREPM (**B**), along with R-Luc, and incubated with or without RA (1 μM) for 8 hours. Data are mean ± SD. Statistical significance was examined by the Student's *t*-test. *, $p < .05$; ***, $p < .005$; NS, not significant ($p = .143$ in **A**, $p = .248$ in **B**). Chromatin immunoprecipitation assays for E14.5 forebrain-derived NPCs (**C**) and freshly prepared P1 forebrain (**D**) were performed using anti-RARα, RARβ, RXR, and control IgG antibody, and followed by polymerase chain reaction with primers targeted to a fragment including the RARE in the *gfap* promoter.

a reporter assay using GF1L-pGL3 in combination with a construct expressing a dominant-negative form of STAT3 (DN-STAT3) in which tyrosine 705 of STAT3 is substituted by phenylalanine [13]. As expected, expression of DN-STAT3 in NPCs suppressed the activation of the *gfap* promoter by LIF (Fig. 2A). Furthermore, DN-STAT3 dramatically inhibited the activation of the promoter induced by simultaneous addition of RA and LIF. We have previously shown that a STAT-binding site (TTCCGAGAA) located 1.5 kb upstream of the *gfap* transcription initiation site is indispensable for STAT3 to activate the *gfap* promoter. When this site was mutated to *CCAA*GAGAA (Fig. 2B), activation of the *gfap* promoter by combined treatment with RA and LIF, as well as with LIF alone, was virtually abolished (Fig. 2B). Collectively, these results reveal that the activation of STAT3 and its binding to the cognate recognition site are essential for the synergistic activation of the *gfap* promoter induced by RA and LIF.

A RARE in the *Gfap* Promoter Is Critical for Synergistic Activation Induced by RA and LIF

We identified a putative RARE site (AGTTCAAGGTCA) located 2.5 kb upstream of the *gfap* transcription start site. To determine whether this RARE is important for the synergistic activation of the promoter by RA and LIF, we next tested the

responsiveness of the deleted *gfap* promoter construct GF1LB, which lacks a 0.6-kb fragment that spans the RARE (Fig. 3A) [13]. It has been shown that, in the absence of ligands, the RAR/RXR heterodimer functions as a transcriptional suppressor by forming a complex with corepressor molecules such as N-CoR and SMRT [20, 24, 41, 42]. Consistent with these findings, the responsiveness of GF1LB to LIF stimulation was augmented relative to GF1L, probably due to deletion of the region containing the RARE. There was no further augmentation of LIF-induced activation of GF1LB by RA stimulation (Fig. 3A). We also obtained similar results to those with the deletion construct when nucleotide substitutions were made in the RARE (AGTT*TGGA*GTCA, GF1L-RAREPM) (Fig. 3B).

We next examined whether RAR/RXR indeed associates with the region of the *gfap* promoter containing the RARE, by chromatin immunoprecipitation (ChIP) assay using specific antibodies against RARα, RARβ, and RXR. As shown in Figure 3C and D, binding of RARα, RARβ, and RXR to the RARE-containing region was detected in cultured NPCs and in the forebrain at postnatal day 1 (P1) when astrocytogenesis is intensively occurring [2, 43]. These results suggest that the RARE in the *gfap* promoter plays a critical role in the synergistic action of RA and LIF.

We then sought to examine whether RA signaling is in fact activated in the P1 brain in vivo. To this end, we introduced luciferase construct containing 3× RARE (pGL3-RARE) to P1 forebrain by electroporation with or without a plasmid expressing dominant negative form of RARα (RAR403) in which transcriptional activation domain is deleted [44]. On the following day, dissociated cells from the forebrain were subjected to a reporter assay. As shown in supporting information Figure 3, we observed an activation of the reporter and this activation was completely inhibited by the expression of RAR403, suggesting that RA signaling is actually activated in vivo during astrocytogenesis.

RA Increases Histone H3 Acetylation Around the STAT-binding Site in the *gfap* Promoter, Thus Enhancing STAT3 Binding to the Promoter

Upon binding of RA to RAR/RXR, the transcriptional repressor complex has been shown to be replaced by coactivator molecules, including p300/CBP, that possess histone acetyltransferase activity [20, 41, 42]. In support of this, we confirmed RA-induced exchange of association factor with RARα by a coimmunoprecipitation assay in the presence or absence of RA in 293T cells transfected with Myc-RARα, N-CoR-FLAG, and p300-HA expressing constructs (supporting information Fig. 4). Since histone acetylation is considered to relax chromatin structure, allowing gene transcription [16, 45], we hypothesized that the mechanism of synergistic action of RA and LIF on the *gfap* promoter might involve an alteration of histone acetylation. To test this hypothesis, we carried out a ChIP assay, using a specific antibody for acetylated histone H3, in NPCs stimulated with RA. As shown in Figure 4B, histone H3 acetylation was enhanced not only in the RARE-containing region but also in the STAT site-containing region of the *gfap* promoter in response to RA; this increased acetylation may enable STAT3 to bind more efficiently to the relaxed promoter. Moreover, we observed an enhancement of LIF-induced STAT3 binding to the *gfap* promoter when the cells were costimulated with RA (Fig. 4C). Thus, these results suggest that RA facilitates STAT3 binding to the promoter through an alteration in chromatin modification.

Since it has been shown that there was an inverse correlation between DNA methylation status of the *gfap* promoter

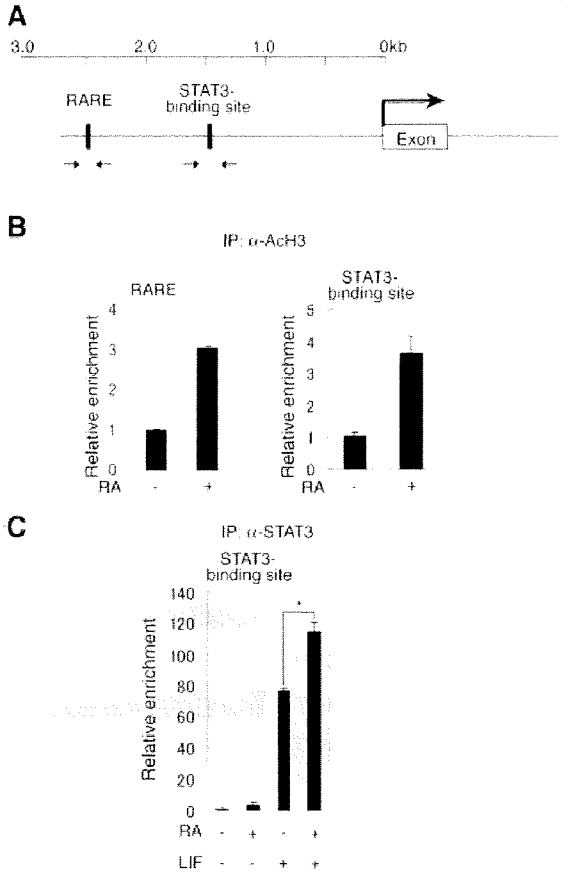

Figure 4. Retinoic acid (RA)-induced histone H3 acetylation in the STAT site-containing region facilitates STAT3 binding to the *gfap* promoter. (**A**): Schematic diagram of the *gfap* promoter showing the locations of the retinoic acid response element (RARE) and STAT3-binding sequences. Arrows indicate the locations of primers used in qPCR for chromatin immunoprecipitation (ChIP) assays in (**B**) or (**C**). Cells were stimulated with or without RA (1 μM) and leukemia inhibitory factor (50 ng/ml) for 20 minutes. ChIP assays were performed using antiacetylated histone H3 and IgG antibodies (**B**), or anti-STAT3 and IgG antibodies (**C**), followed by polymerase chain reaction with primers targeted to fragments including the RARE or STAT3-binding site in the *gfap* promoter as indicated. Data are mean ± SD. Statistical significance was examined by the Student's *t*-test. *, $p < .05$.

containing STAT3 binding site and the potential of cells to express *gfap* [4, 46, 47], we next examined whether methylation of the promoter region was affected by RA stimulation using bisulfite sequence method. However, in agreement with previous reports [4, 46, 47], almost all CpG sites at *gfap* promoter had become almost demethylated in 4-day-cultured NPCs, and this was not further changed even after additional 2-day culture with RA (data not shown).

Histone Acetylation Promoted by HDAC Inhibition Mimics the Effect of RA on Astrocytic Differentiation of NPCs

To further explore the relationship between histone acetylation and astrocytic differentiation of NPCs, we sought to determine whether treatment with the HDAC inhibitor valproic acid (VPA; 2-propylpentanoic acid) [48] affects GFAP-positive astrocyte differentiation of NPCs. Although VPA

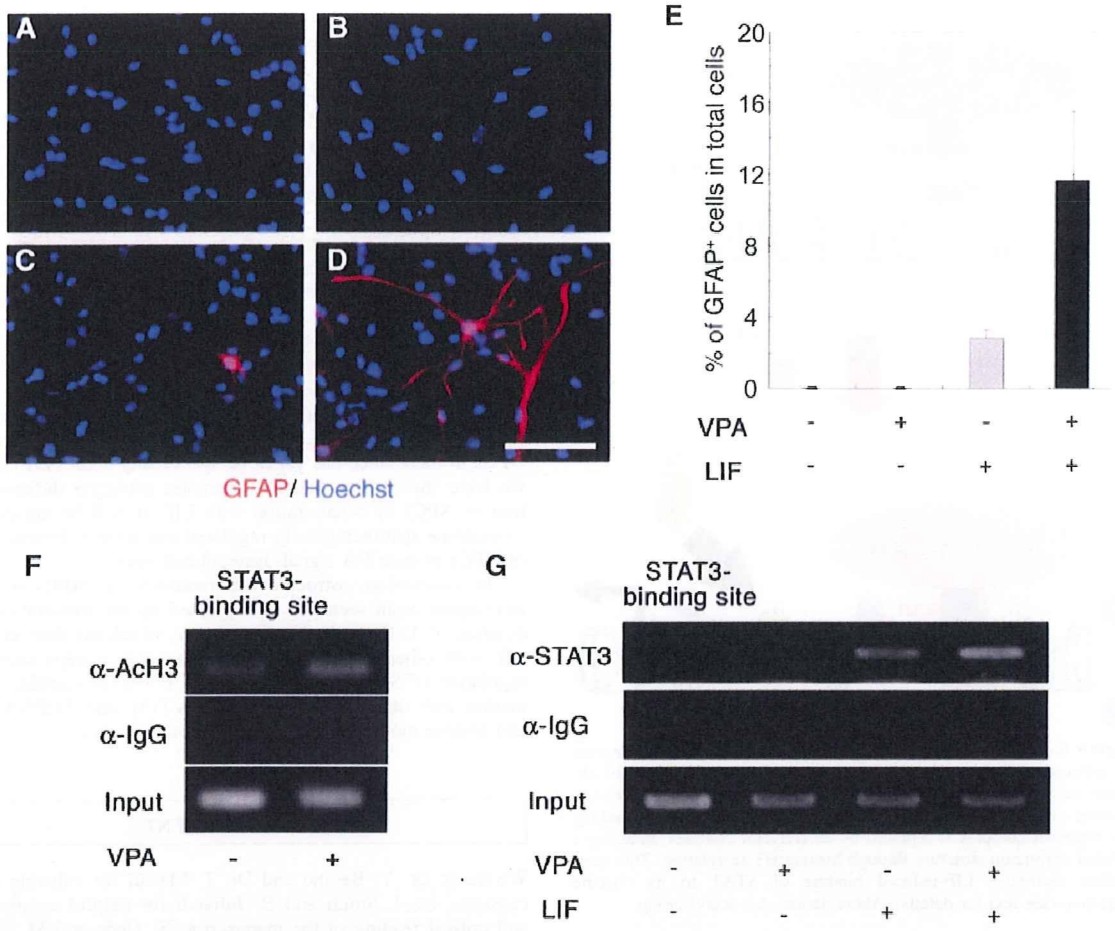

Figure 5. The histone deacetylases inhibitor valproic acid (VPA) promotes leukemia inhibitory factor (LIF)-induced astrocyte differentiation of neural precursor cells. Cells were cultured with medium alone **(A)**, VPA (1 mM) **(B)**, LIF (50 ng/ml) **(C)**, or VPA (1 mM) plus LIF (50 ng/ml) **(D)** for 2 days, and then stained with an antibody against glial fibrillary acidic protein (GFAP; red) and with Hoechst 33258 (blue). Scale bar = 50 μm. **(E):** Percentage of GFAP-positive cells in total cells was calculated. Data are mean ± SD. Chromatin immunoprecipitation assays were performed using anti-acetylated histone H3 and IgG antibodies **(F)**, or anti-STAT3 and IgG antibodies **(G)**, and followed by polymerase chain reaction with primers targeted to a fragment including the STAT3-binding sequence within the *gfap* promoter.

itself did not induce GFAP-positive cells, we observed that VPA and LIF synergistically induced GFAP-positive astrocyte differentiation of NPCs (Fig. 5A–E), as in the case of RA and LIF. We further confirmed that histone H3 acetylation around the STAT3-binding site was increased by VPA treatment in NPCs (Fig. 5F). Finally, we tested the association of STAT3 with the *gfap* promoter by ChIP assay, and found that STAT3 bound more effectively to the promoter in the presence of both VPA and LIF than with LIF alone (Fig. 5G). Taken together, these results suggest that histone acetylation enhances STAT3 binding to the *gfap* promoter and thereby plays an important role in astrocyte differentiation of NPCs that have been synergistically induced by RA and LIF.

Discussion

It was reported recently that, at relatively late gestation, RA promotes astrocyte differentiation of NPCs induced by ciliary neurotrophic factor (CNTF), a member of the IL-6 cytokine family that activates the same gp130-JAK-STAT pathway as does LIF [49]. However, a mechanism to explain this function of RA has yet to be presented. In this study, we have shown that RA synergistically induces astrocyte differentiation of NPCs in cooperation with LIF, a plausible explanation for which is that RA enhances histone H3 acetylation around the STAT3-binding site in the *gfap* promoter, thus making the site more accessible to STAT3 (Fig. 6). Moreover, we found that histone acetylation induced by VPA also promoted LIF-induced astrocyte differentiation. Taken together, these results indicate that RA-induced alteration of histone acetylation regulates astrocyte differentiation of NPCs by facilitating STAT3 binding to the astrocyte-specific gene promoter. In this context, O'Donnell et al. [50] have recently shown that histone acetylation induced by the ETS domain transcription factor ELK-1 stimulates recruitment of nuclear factor IA to the *c-fos* gene promoter. Taking their and our findings into consideration, this type of mechanism (i.e., primary effectors trigger a HAT relay switch, which facilitates the recruitment of additional transcription factors) may be widespread in histone acetylation-associated gene activation.

We further found that RARα, RARβ, and RXR associate with a RARE-containing region of the *gfap* promoter, and